UNIVERSITÄT DES SAARLANDES

Variational Quantum Algorithms for State Preparation and Dynamics Simulations of Many-Body Models

Peter P. Orth (Saarland University)

Seminar, Desy Center for Quantum Technologies and Applications, 18 June 2024

References:

- J. C. Getelina *et al.*, arXiv:2404.09132 (2024).
- A. C. Y. Li *et al.*, Phys. Rev. Research 5, 033071 (2023)
- B. McDonough *et al.*, 2022 IEEE Workshop on Quantum Computing Software
- I-C. Chen *et al.*, Phys. Rev. Research 4, 043027 (2022); I.-C. Chen et al. arXiv:2310:03924

The future is quantum, but how?

- Quantum Processing Units (QPUs) will likely be special purpose units like GPUs
- Leverage access to wavefunctions that are impossible to represent classically
  - Sampling output from their probability distributions of bitstrings
  - Measure correlation functions inaccessible otherwise
  - Simulate complex dynamics and monitor observables
  - Use information about wavefunction to reduce problem instance: quantum-informed data reduction

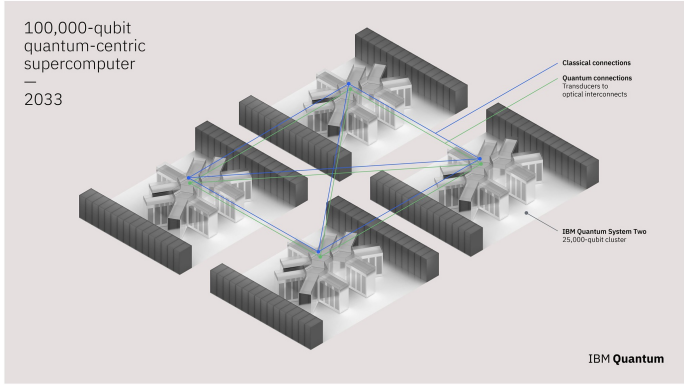

A visual rendering of IBM Quantum's 100,000-qubit quantum-centric supercomputer, expected to be deployed by 2033. (Credit: IBM)

Quantum-centric supercomputing: largely open question how it will look like. Depends also when and how will QEC be possible?

The quantum present: variational quantum algorithms for noisy hardware

UNIVERSITÄT DES SAARLANDES

- General goal: Extract computational power from noisy quantum computers
- VQAs are tailored to hardware capabilities and limitations
- Approach: Prepare states that cannot be efficiently prepared classically
- Combine with classical resources in hybrid quantum-classical algorithms
- Examples from quantum many-body systems' simulations
  - Ground states in dimensions $d > 1$, highly excited states in any d (volume law entangled)
  - Thermal states and response functions at intermediate temperatures
  - Nonequilibrium dynamics: quenches, driven (open) systems, nonlinear response
- Focus here on studies executed on real quantum hardware

Main Collaborators

- Thomas Iadecola (Iowa State University)
- Yong-Xin Yao (Ames National Lab)

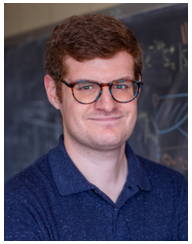
T. Iadecola


Y. Yao

- Collaborators at the “Superconducting Quantum Materials and Systems” Center of the U.S. Department of Energy

SQMS SUPERCONDUCTING QUANTUM MATERIALS & SYSTEMS CENTER


P. Sharma


J. Getelina


N. F. Berthusen

UNIVERSITÄT DES SAARLANDES

Students and postdocs

- Prachi Sharma (Saarland Univ)
- Joao Getelina (Ames National Lab)
- Noah F. Berthusen (Univ Maryland)
- I-Chi Chen (Iowa State Univ)
- Benjamin McDonough (Yale)


I-C. Chen


B. McDonough

Ground state preparation using quantum computers

Ground state preparations using VQAs

Variational quantum eigensolver (VQE)

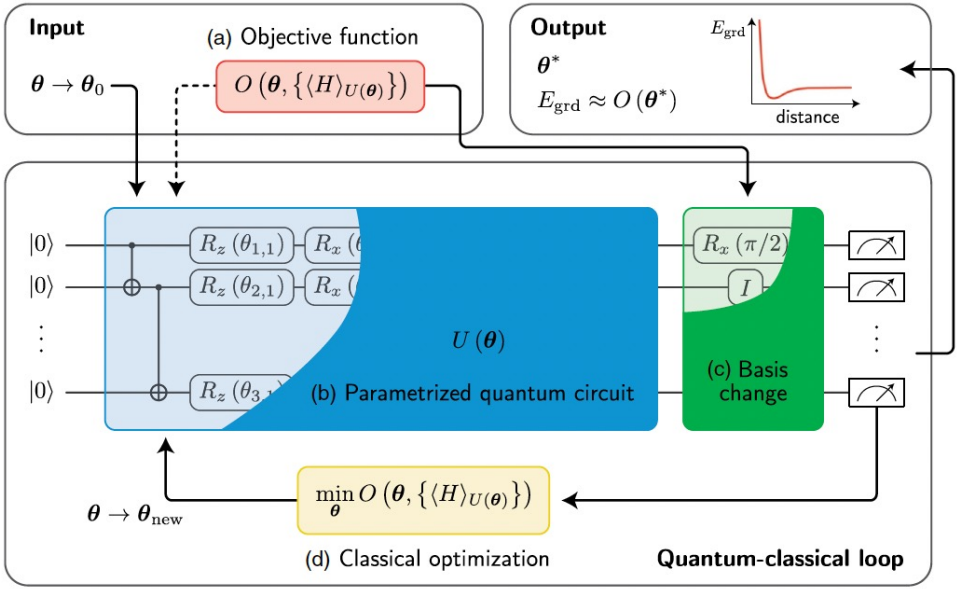

From Bharti et al, RMP (2022)

Example: Kitaev spin model in magnetic field

$$H_K = -J_x \sum_{x \text{ bonds}} X_i X_j - J_y \sum_{y \text{ bonds}} Y_i Y_j - J_z \sum_{z \text{ bonds}} Z_i Z_j,$$

$$H = H_K + \sum (h_x X_i + h_y Y_i + h_z Z_i),$$

Frustrated spin model on trivalent graph

➢ maps well to Rigetti Aspen QPU geometry

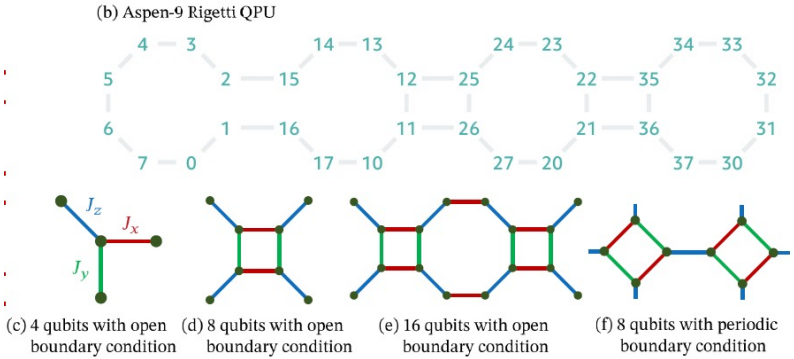

(c) 4 qubits with open boundary condition (d) 8 qubits with open boundary condition (e) 16 qubits with open boundary condition (f) 8 qubits with periodic boundary condition

Li, PPO et al., PRR (2023)

Ground State Preparation using QITE

Variational ansatz form with Paulis A_μ

$$|\Psi[\boldsymbol{\theta}]\rangle = \prod_{\mu=0}^{N_{\boldsymbol{\theta}}-1} e^{-i\theta_\mu \hat{\mathcal{A}}_\mu} |\Psi_0\rangle$$

- Variational parameters evolve in time according to equation of motion
- Ansatz expands during time evolution to maintain required expressivity

$$\frac{d\boldsymbol{\theta}}{d\tau} = \mathbf{M}^{-1}\mathbf{V}.$$

Quantum metric M and gradient V measured on QPU (direct measurement and Hadamard circuits with control-Pauli)

- Quantum imaginary time evolution (QITE) can be implemented on quantum computers, e.g.
  - Rewrite Trotter time step as unitary [1]
  - Embed in unitary using ancillary qubit(s) [2]
  - Equation of motion technique using MacLachlan's principle [3, 4]
- Adaptive variational QITE (AVQITE)
  - Expands variational ansatz during computation
  - Ensures MacLachlan distance b/w exact and variational time evolution remains below fixed threshold
  - Guaranteed to converge to the ground state

[1] Motta et al., Nat. Phys. (2020); [2] Lin et al., PRX Q (2022); [3] McArdle et al., npj QI (2019); [4] Gomes, PPO et al., Adv QT (2021)

Benchmarking VQE using the Kitaev spin model

- Rich phase diagram in field with non-abelian phase

$$H = H_K + \sum_i (h_x X_i + h_y Y_i + h_z Z_i),$$

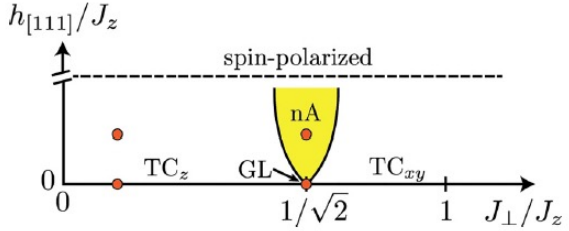

- Hamiltonian Variational Ansatz (HVA): $U(\vec{\theta}) = U_{\mathrm{HVA}}(\vec{\theta}_L) U_{\mathrm{HVA}}(\vec{\theta}_{L-1}) \cdots U_{\mathrm{HVA}}(\vec{\theta}_1).$

Circuit of a single layer of the HVA ansatz

$$U_{\mathrm{HVA}}(\vec{\theta}_\ell) = e^{-i\theta_{\ell;6}\sum_i Z_i} e^{-i\theta_{\ell;5}\sum_{z\ \mathrm{bonds}} Z_i Z_j} \times e^{-i\theta_{\ell;4}\sum_i Y_i} e^{-i\theta_{\ell;3}\sum_{y\ \mathrm{bonds}} Y_i Y_j} \times e^{-i\theta_{\ell;2}\sum_i X_i} e^{-i\theta_{\ell;1}\sum_{x\ \mathrm{bonds}} X_i X_j}.$$

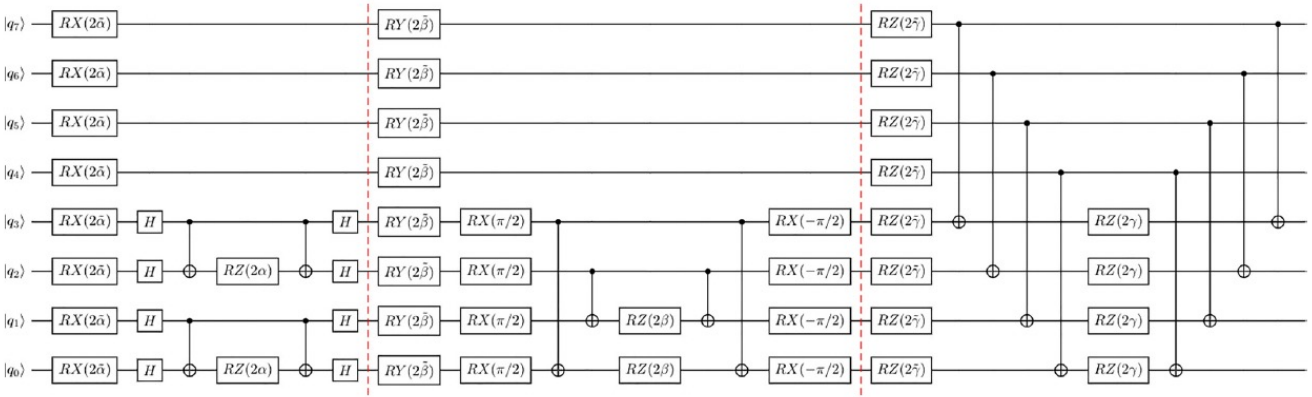

FIG. 3. HVA with one layer on eight qubits. The Hamiltonian variational *Ansatz* (HVA) with one layer on eight qubits splits into

Li, PPO et al., PRR (2023)

Required depth of variational ansatz

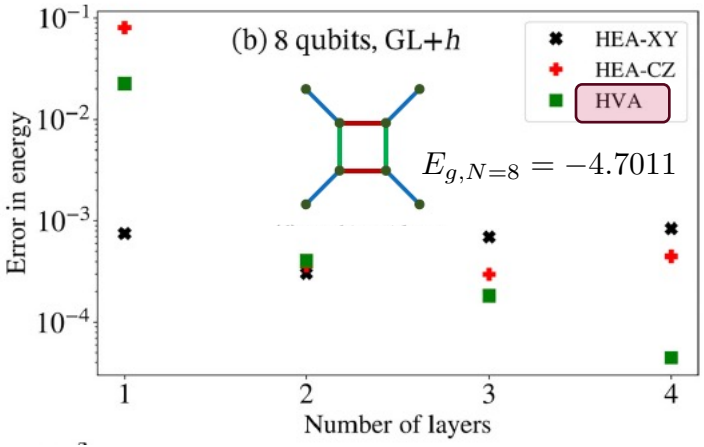

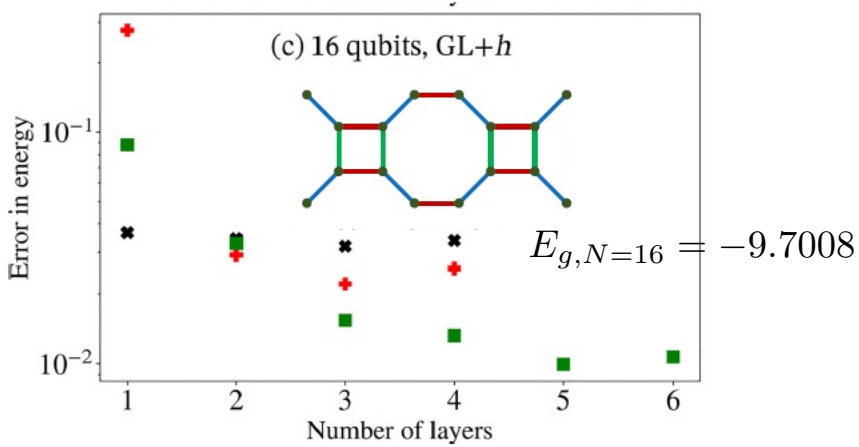

- Error in energy decreases with layer number ➢ 4-layer HVA sufficient for 16 spins
  - Number of entangling gates per layer = 2 * number of bonds = 16 (for 8 spins) and 36 (for 16 spins)
- Number of variational parameters:
  - Proportional to layer number = 6 parameters per layer
  - Independent of system size (advantage of original HVA)

Single layer unitary of HVA:

$$U_{\mathrm{HVA}}(\vec{\theta}_\ell) = e^{-i\theta_{\ell;6}\sum_i Z_i} e^{-i\theta_{\ell;5}\sum_{z\ \mathrm{bonds}} Z_i Z_j} \times e^{-i\theta_{\ell;4}\sum_i Y_i} e^{-i\theta_{\ell;3}\sum_{y\ \mathrm{bonds}} Y_i Y_j} \times e^{-i\theta_{\ell;2}\sum_i X_i} e^{-i\theta_{\ell;1}\sum_{x\ \mathrm{bonds}} X_i X_j}.$$

Statevector simulation results

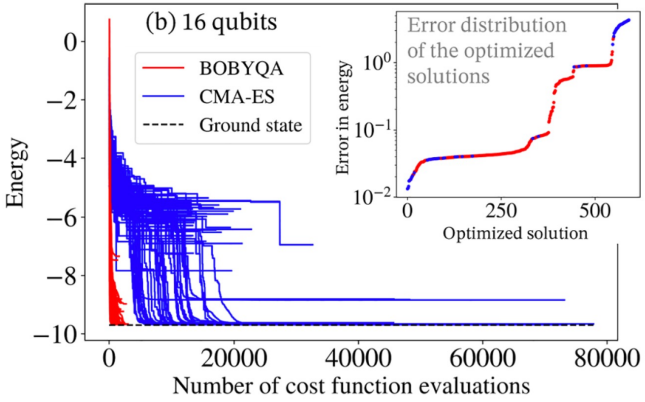

- 16 spins at gapless point + h field with 4-layer HVA
- Use multiple initial values, mixed optimizers

Optimizer	Gradient-free	Genetic	Local
BFGS	×	×	✓
BOBYQA [91]	✓	×	✓
CMA-ES [95]	✓	✓	×

Qubits	Optimizer	Error in energy	Cost function evaluations
8	BFGS, 501 initial values	0.00094	Mean, 5352; max, 10865
16	BFGS, 501 initial values	0.02672	Mean, 5569; max, 10186
8	BOBYQA, 501 initial values	0.00045	Mean, 1099; max, 1920
16	BOBYQA, 501 initial values	0.01744	Mean, 1255; max, 3049
8	CMA-ES	0.00015	43290
16	CMA-ES	0.04036	49335
8	CMA-ES, 80 initial values	0.00005	Mean, 20528; max, 83590
16	CMA-ES, 80 initial values	0.01327	Mean, 27504; max, 73138

Correlation functions and energy gap with statevector

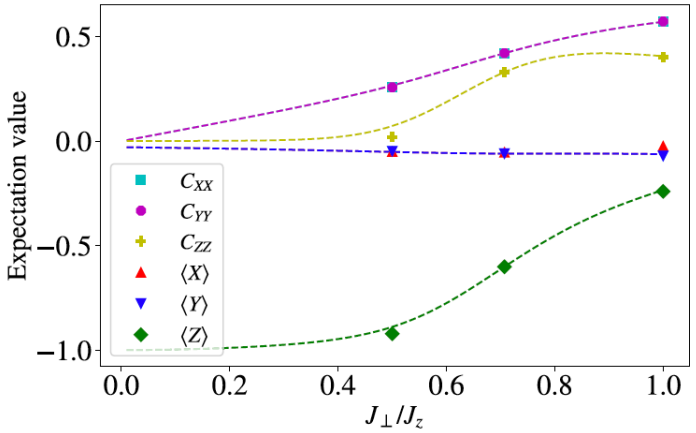

$$C_{\alpha\alpha} = \langle \alpha_j \alpha_k \rangle - \langle \alpha_j \rangle \langle \alpha_k \rangle \ \ (\alpha = X, Y, Z)$$

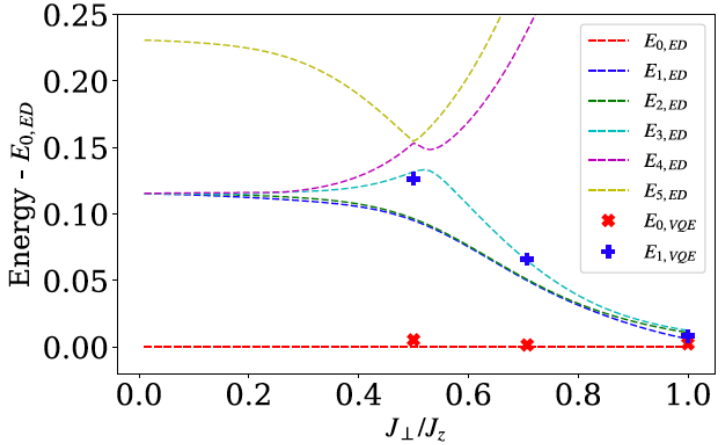

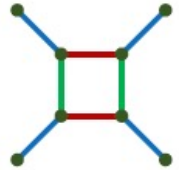

(d) 8 qubits with open boundary condition

- 8-spin model in magnetic field using 8-layer HVA
  - More layers needed to also represent first excited state
- Optimal solution of CME-ES (480 initial values) & BOBYQA (3001 initial values)
- Gap closing well captured within VQE, even though VQE tracks 2nd excited level

Results including shot noise

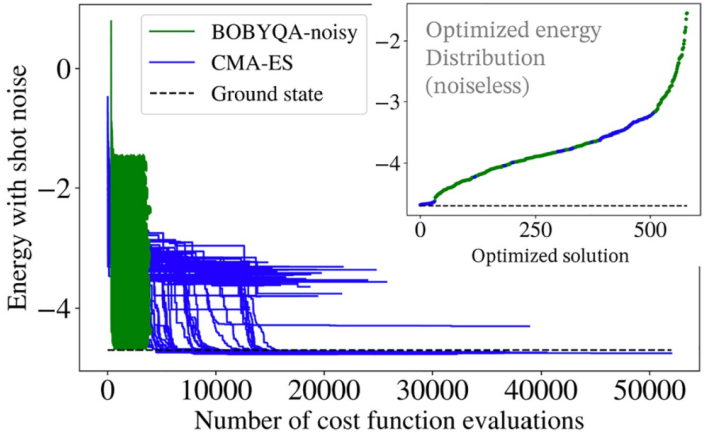

- 8-spin model with 4-layer HVA
- 8000 measurement shots
- Std. deviation of optimized energy = 0.02
- CMA-ES (80 init.) and BOBYQA (501 init.)

Optimizer	$E_{\text{noiseless}} - E_0$	$E_{\text{noisy}} - E_0$	Cost function evaluations
BFGS, 501 initial values	0.45069	0.42052	Mean, 747; max, 1994
BOBYQA, 501 initial values	0.27485	0.21843	Mean, 471; max, 610
BOBYQA-noisy, 501 initial values	0.07989	−0.00453	Mean, 3532; max, 4004
CMA-ES	0.02416	−0.06462	37570
CMA-ES, 80 initial values	0.01610	−0.07125	Mean, 21042; max, 52000

Executing optimized ansatz on Aspen-9 QPU

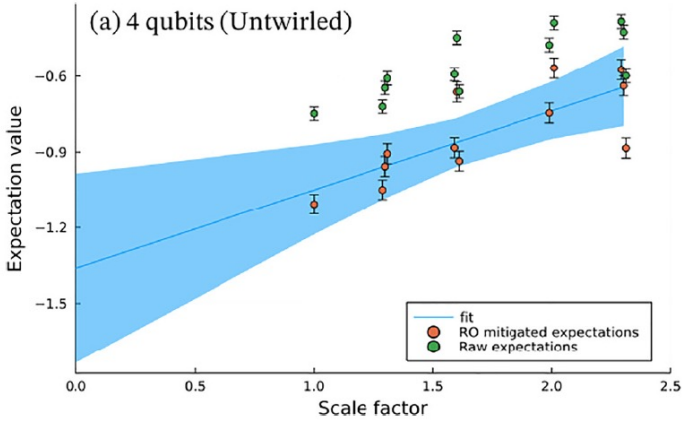

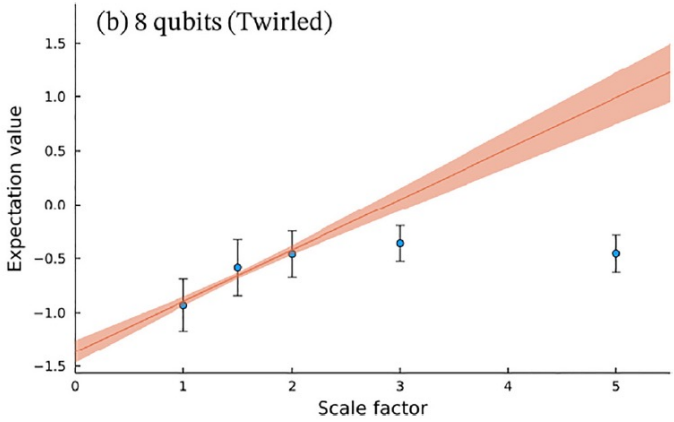

Pauli twirling of 2-qubit gates

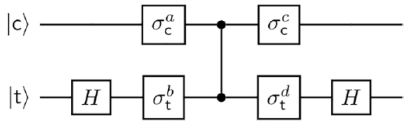

- With zero-noise extrapolation (ZNE) and readout error mitigation
- 4-qubit result within one standard deviation of true value = -1.583
- 8-qubit result is far off from exact value = -4.23
  - Circuit contains $N = 16 \times (\text{Scale factor})$ CZ gates → exceeds coherence time on hardware at that time (hardware runs executed in 2021)

Quantum Subspace Expansions: going beyond plain VQE

UNIVERSITÄT DES SAARLANDES

- Challenges of hybrid quantum-classical loop in VQE
  - Requires many circuit executions. BOBYQA-noisy: $500 \times 3500 \times N_s = 1.75 \times 10^6 \, N_s$
  - Optimization of noisy energy often landscape difficult
- Alternative: Quantum Subspace Expansions
  - Here we combine HVA-VQE with the Iterative Quantum Assisted Eigensolver (IQAE) [1]
  - Measure Hamiltonian in "low-energy" Krylov subspace on a quantum computer
  - Diagonalize the Krylov-basis Hamiltonian matrix on a classical computer

Expand state in fine-grained Krylov subspace (FGKS): $\mathbb{CS}_K \equiv \{P_j|\Psi_{\mathrm{VQA}}\rangle\}_{P_j \in \cup_{l=0}^{k} \mathbb{H}^l}$

$$|\Phi\rangle = \sum_i a_i P_i |\Psi_{\mathrm{VQA}}\rangle$$

Spans Moment-K FGKS

Pauli strings in $\cup_{l=0}^{k} \mathbb{H}^l$

Set of Pauli strings in l-th power of the Hamiltonian

Bharti, Haug PRA (2021)

Iterative Quantum Assisted Eigensolver

- Measure Hamiltonian $H = \sum_k c_k P_k$ and overlap matrices S_{ij} in Krylov subspace

$$(H)_{ij} = \sum_k c_k \langle \Psi_{\mathrm{VQA}} | P_i P_k P_j | \Psi_{\mathrm{VQA}} \rangle$$

$$(S)_{ij} = \langle \Psi_{\mathrm{VQA}} | P_i P_j | \Psi_{\mathrm{VQA}} \rangle$$

  - Obtain on quantum hardware
  - Use low-depth VQA
  - Group Paulis into commuting sets

$$\mathbb{CP}_K \equiv \{\hat{P}_i \hat{P}_k \hat{P}_j\}^{\hat{P}_k \in \cup_{k=0}^{1} \mathbb{P}_k}_{\hat{P}_i, \hat{P}_j \in \cup_{k=0}^{K} \mathbb{P}_k}$$

- Solve generalized eigenvalue problem in Krylov subspace

$$\sum_{ijk} H_{ij} V_{jk} = \sum_{ijk} S_{ij} V_{jk} \lambda_k$$

Diagonal matrix of eigenvalues

Matrix of eigenvectors in Krylov basis $V_{jk} \equiv (V_k)_j \in \mathbb{CS}_K \equiv \{P_j | \Psi_{\mathrm{VQA}} \rangle\}_{P_j \in \cup_{l=0}^{k} \mathbb{H}^l}$

Bharti, Haug PRA (2021); See also McClean et al, PRA (2017).

Benchmark Paired IQAE on nonintegrable spin model

UNIVERSITÄT DES SAARLANDES

- Benchmark on nonintegrable transverse & mixed field Ising models

$$H = J \sum_{\langle i,j \rangle} Z_i Z_j + h_x \sum_i X_i + h_z \sum_i Z_i$$

- HVA ansatz of depth L: $\prod_{\ell=1}^{L} e^{-i\theta_{\ell,x} \sum_i X_i} e^{-i\theta_{\ell,z} \sum_i Z_i} e^{-i\theta_{\ell,zz} \sum_{\langle i,j \rangle} Z_i Z_j} |+\rangle^{\otimes N}$
- Balance quantum and classical resources: Paired IQAE = PIQAE
  - HVA depth L: sets depth of quantum circuit and VQE cost
  - Dimension of moment-K Krylov subspace: sets measurement cost and size of subspace matrix
- Parameter sets: Strongly nonintegrable point in MFIM, close to criticality in TFIM
- Compare error of PIQAE ground state energy to exact diagonalization

Scaling of quantum measurement cost

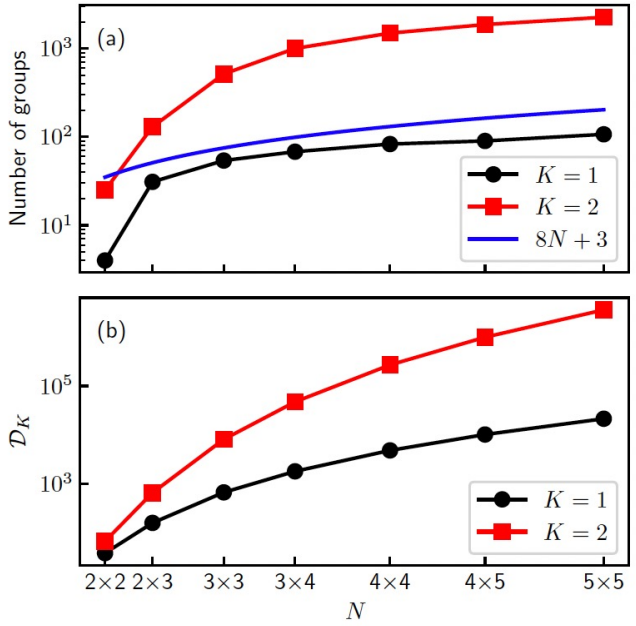

FIG. 1. **System-size dependence of the number of groups of commuting Pauli strings in $\mathbb{CP}_K$ for the 2D TFIM.** (a) Number of self-commuting groups N_g of Pauli

- Quantum resources given by number of self-commuting Pauli groups N_g that need to be measured
- N_g scales linearly with system size N for TFIM
- Obtain N_g from $\mathcal{D}_K = |\mathbb{CP}_K|$ by greedy coloring algorithm (NP-hard graph coloring)

$$\mathbb{CP}_K \equiv \left\{ \hat{P}_i \hat{P}_k \hat{P}_j \right\}_{\hat{P}_i, \hat{P}_j \in \cup_{k=0}^{K} \mathbb{P}_k}^{\hat{P}_k \in \cup_{k=0}^{1} \mathbb{P}_k}$$

Pauli expectation values needed up to moment-K

Balance quantum and classical resources

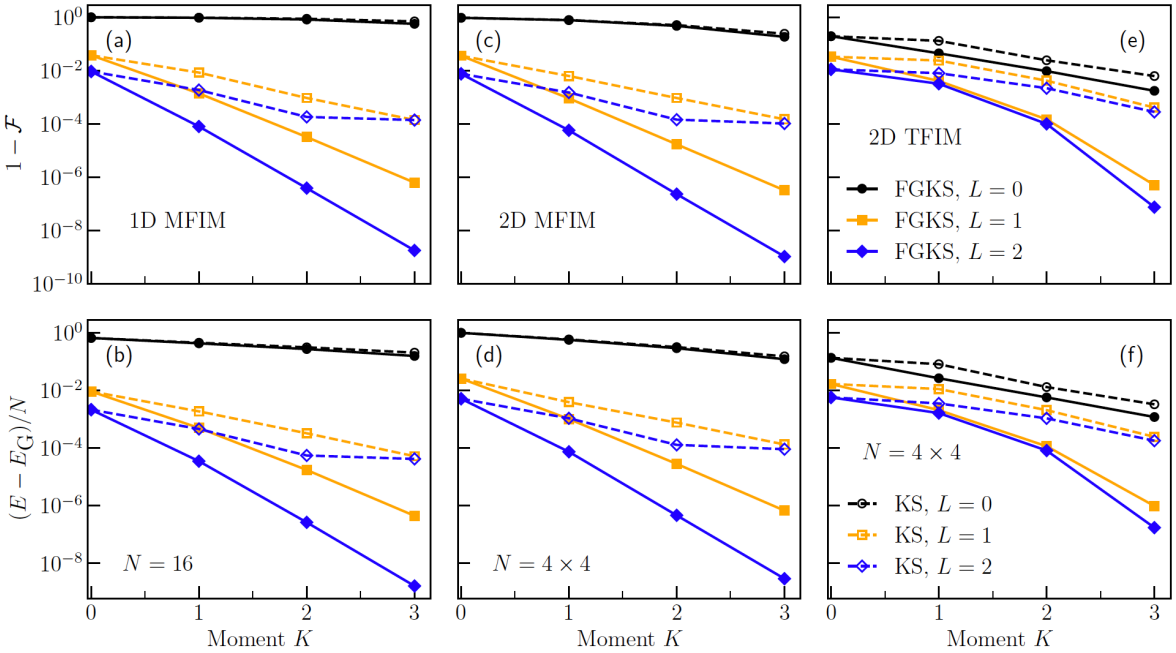

- Statevector simulations
- Fidelity & energy of Krylov ground state compared to ED
- More rapid convergence for deeper HVA ansatz
- Fine-grained Krylov basis performs better
- Same quantum resources for FGKS and KS

$$\mathrm{FGKS} \equiv \mathbb{CS}_K \equiv \{P_j|\Psi_{\mathrm{VQA}}\rangle\}_{P_j \in \cup_{l=0}^{k} \mathbb{H}^l}$$

$$\mathrm{KS} \equiv \{H^j|\Psi_{\mathrm{VQA}}\rangle\}_{j=0}^{K}$$

J. C. Getelina et al., arXiv:2404.09132 (2024).

Shot noise results of 4 x 4 TFIM

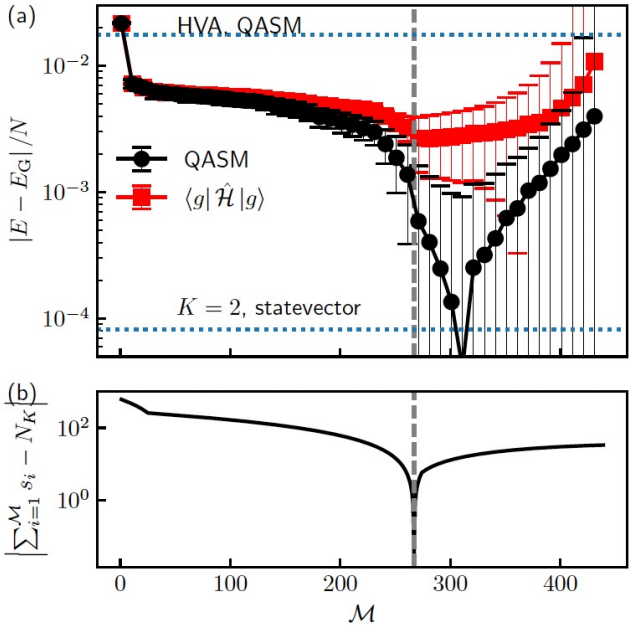

2^{14} measurement shots. Error bars are standard deviations based on 10 sets of noisy H_{ij} and S_{ij} obtained from sampling Pauli expectation values from distribution with measured mean and standard errors.

- VQE ansatz is $L = 1$ HVA
- Subspace expansion to moment $K = 2$
- Numerical procedure
  - Obtain noisy H_{ij} and S_{ij} on QPU
  - Perform SVD of S_{ij} and sort singular values $s_1 \geq s_2 \geq \cdots$
  - Use basis spanned by vectors with largest M singular values
  - Transform and diagonalize H_{ij} in this subspace
  - Output lowest energy eigenvalue E_g (black) and state |g>
  - Use $\langle g|\hat{\mathcal{H}}|g\rangle$ as additional figure of merit (true energy of |g>)

Shot noise results of 4 x 4 TFIM

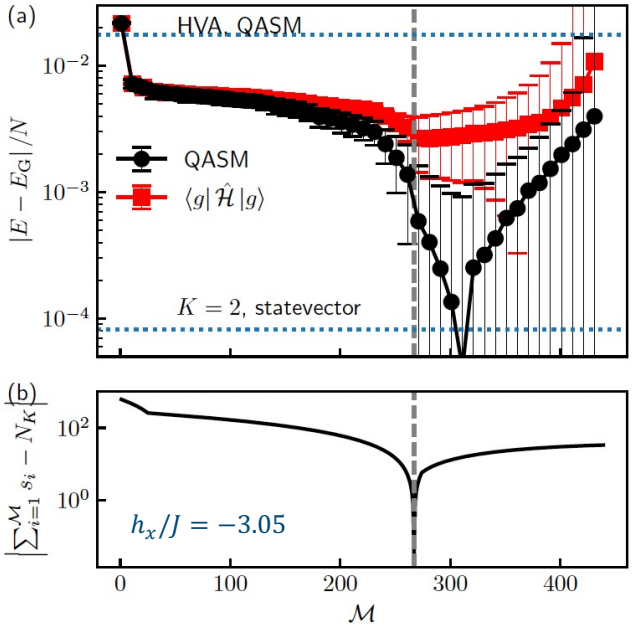

2^{14} measurement shots. Error bars are standard deviations based on 10 sets of noisy H_{ij} and S_{ij} obtained from sampling Pauli expectation values from distribution with measured mean and standard errors.

- VQE ansatz is $L = 1$ HVA
- Subspace expansion to moment $K = 2$
- Numerical procedure
  - Obtain noisy H_{ij} and S_{ij} on QPU
  - Perform SVD of S_{ij} and sort singular values $s_1 \geq s_2 \geq \cdots$
  - Use basis spanned by vectors with largest M singular values
  - Transform and diagonalize H_{ij} in this subspace
  - Output lowest energy eigenvalue E_g (black) and state |g>
  - Use $\langle g|\hat{\mathcal{H}}|g\rangle$ as additional figure of merit (true energy of |g>)
- Challenge: Noise renders zero singular values of S_{ij} finite
  - Energy shows minimum at intermediate M
  - How to determine optimal M_o, i.e. select size of Krylov basis?

New parameter-free convergence criterion

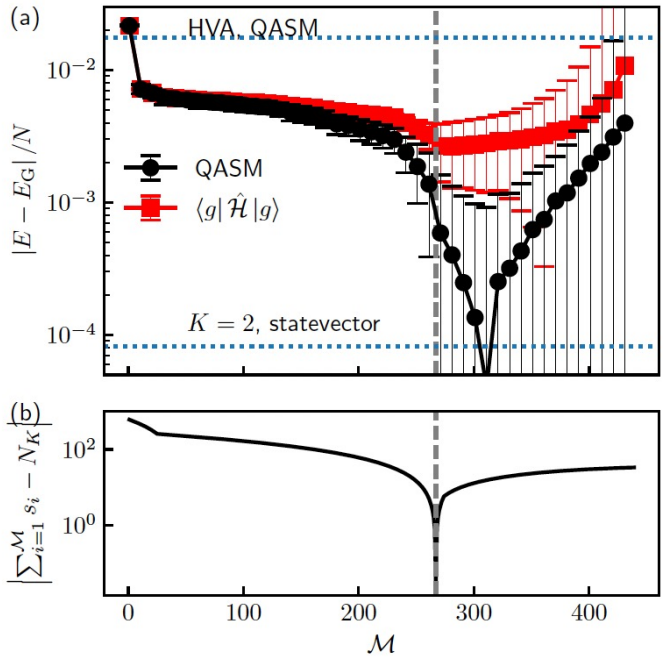

FIG. 3. **QASM simulator results for 4×4 TFIM** (a)

- We propose new convergence criterion based on preserving the trace of the overlap matrix S_{ij}
- Without noise: $\mathrm{Tr}(S) = N_K$
- With noise, we select optimal M via

$$\mathcal{M}_o = \min_{\mathcal{M}} \left| \sum_{i=1}^{\mathcal{M}} s_i - N_K \right|$$

2^{14} measurements. Error bars are standard deviations.

PIQAE results on hardware: 5-site MFIM on `ibm_quito`

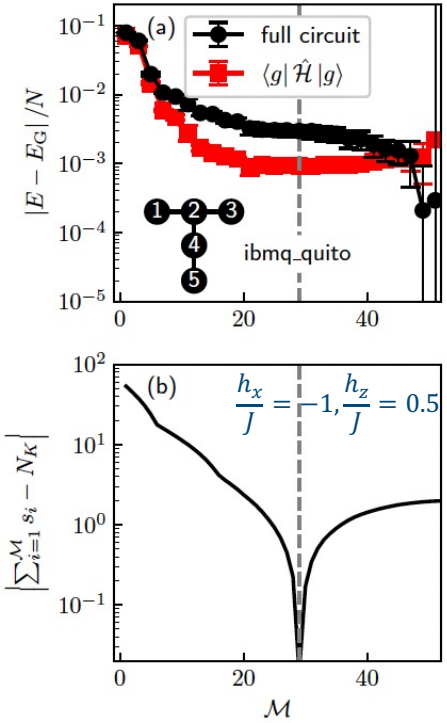

2^{14} measurements. Error bars are standard deviations.

- HVA with $L = 1$, FGKS moment $K = 2$
- $N_g = 142$ measurement circuits for $|D_{K=2}| = 822$ Pauli expectation values contained up to H^5
- Error improves to $\varepsilon = 3\times10^{-3}$ by more than an order of magnitude compared to HVA $\varepsilon_{HVA} = 0.13$.
- True energy exhibits minimum at M_o

Model	Backend	K	L	$\varepsilon(\mathcal{M}_o)$	$\varepsilon_{rel}(\mathcal{M}_o)$
4×4 TFIM	QASM	2	1	$1(1)\times10^{-3}$	0.03(3)%
5-site MFIM	`ibm_quito`	2	2	$2.9(6)\times10^{-3}$	0.18(4)%

PIQAE results for 16-site MFIM on `ibm_guadalupe`

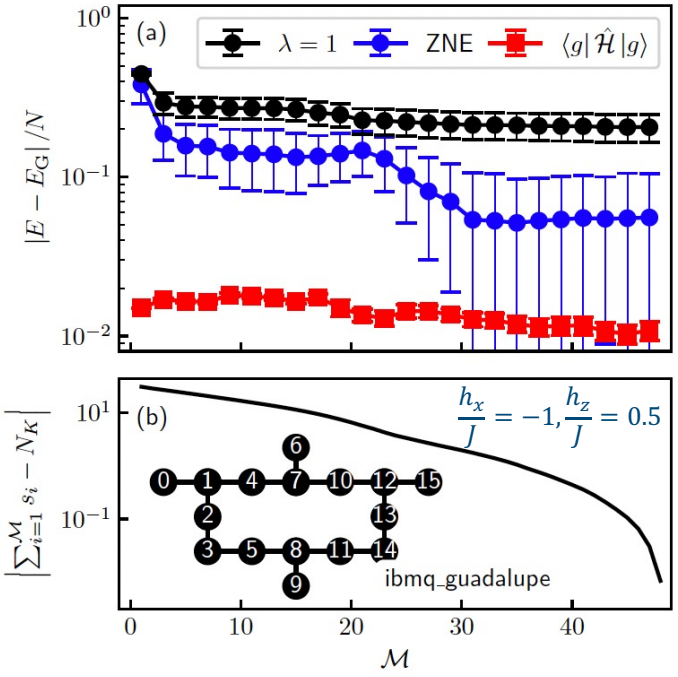

- HVA with $L = 1$, FGKS moment $K = 1$
- $N_g = 83$ measurement circuits for $|D_{K=2}| = 14672$ Paulis
- Twirled readout error mitigation (TREX), DD, Pauli Twirling (32 twirled instances, 2^{14} shots each)
- Noisy result saturates at error $\varepsilon = \frac{|E-E_G|}{N} = 0.21$
- HVA $L = 1$ exhibits $\varepsilon = 0.53$
- ZNE on E with 5 noise levels $1 \leq \lambda \leq 2$ yields $\varepsilon = 0.05$

Model	Backend	K	L	$\varepsilon(\mathcal{M}_o)$	$\varepsilon_{rel}(\mathcal{M}_o)$
4×4 TFIM	QASM	2	1	$1(1) \times 10^{-3}$	0.03(3)%
5-site MFIM	`ibm_quito`	2	2	$2.9(6) \times 10^{-3}$	0.18(4)%
16-site MFIM	`ibm_guadalupe`	1	1	0.05(4)	3(2)%

[TREX] van den Berg et al., PRA (2022); [ZNE] Temme et al., PRL (2017); [ZNE Mitiq] La Rose et al., Quantum (2022).

PIQAE results for 16-site MFIM with Probabilistic Error Reduction

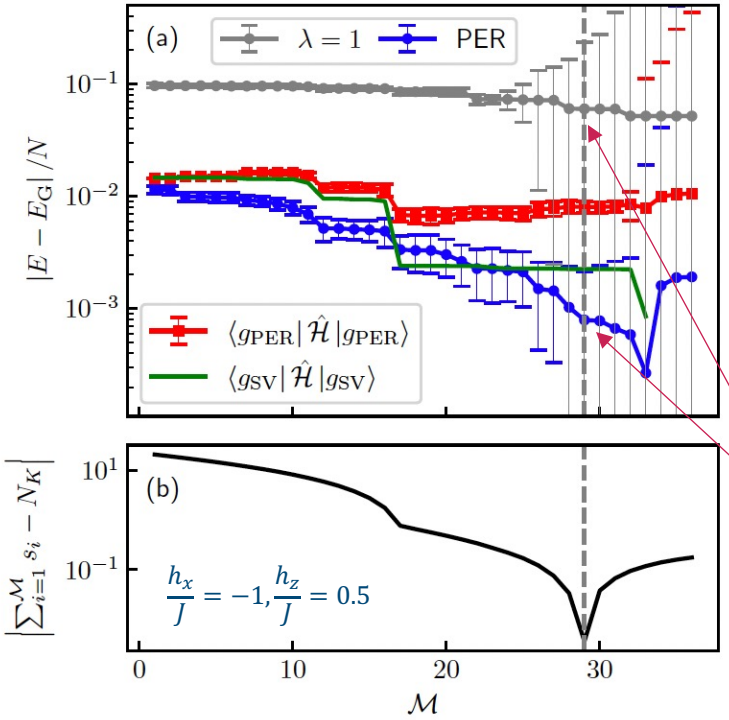

- Run on noisy simulator `fake_guadalupe`
- Same parameters: $L = 1$, $K = 1$, $N_g = 83$
- Pauli noise spectroscopy using RB circuits [1]
  - 150 Pauli twirl samples (50 for pairs, 100 for singles)
  - Depth ([2,4,8,16] with 1000 shots each
- PER with $0 \leq \lambda \leq 1.5$ with 1000 shots each
  - ZNE on each element of H_{ij} and S_{ij}
- PER reduces error by two orders of magnitude

Model	Backend	K	L	$\varepsilon(\mathcal{M}_0)$	$\varepsilon_{rel}(\mathcal{M}_0)$
16-site MFIM	`ibm_guadalupe`	1	1	0.05(4)	3(2)%
16-site MFIM	`fake_guadalupe`	1	1	$1(1) \times 10^{-3}$	0.06(6)%

[1] van den Berg et al., Nat. Phys. (2023);

PIQAE results for 16-site MFIM with Probabilistic Error Reduction

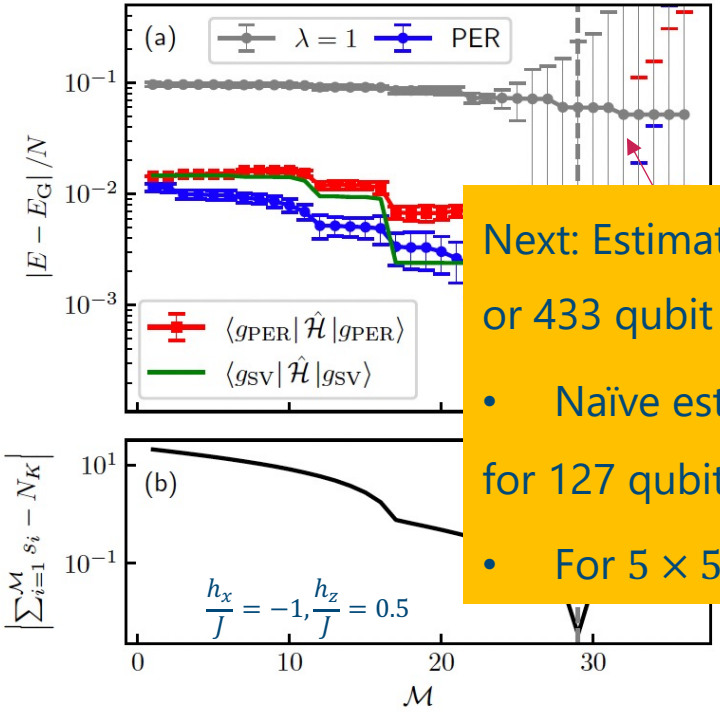

- Run on noisy simulator `fake_guadalupe`
- Same parameters: $L = 1$, $K = 1$, $N_g = 83$

Next: Estimate resources to scale up to to 127 qubit `ibmq_kyiv` or 433 qubit `ibmq_seattle` QPUs.

- Naïve estimate yields 11M Paulis and 62K groups to measure for 127 qubit `ibmq_kyiv`.
- For 5 × 5 TFIM, we find 3.5M Paulis and 2258 groups.

Model	Backend	K	L	$\varepsilon(\mathcal{M}_o)$	$\varepsilon_{rel}(\mathcal{M}_o)$
16-site MFIM	`ibm_guadalupe`	1	1	0.05(4)	3(2)%
16-site MFIM	`fake_guadalupe`	1	1	$1(1) \times 10^{-3}$	0.06(6)%

[1] van den Berg et al., Nat. Phys. (2023);

Open-source software for automated error mitigation

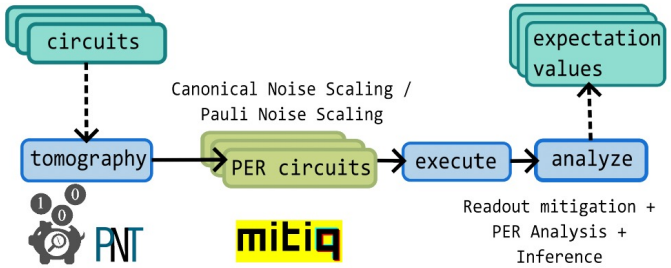

Fig. 1: Illustration of automated error mitigation protocol starting from user defined circuits and returning noise-mitigated expectation values. It includes a noise tomography step involving PNT or GST, whose results are used to generate sampled PER circuits via canonical or Pauli noise scaling.

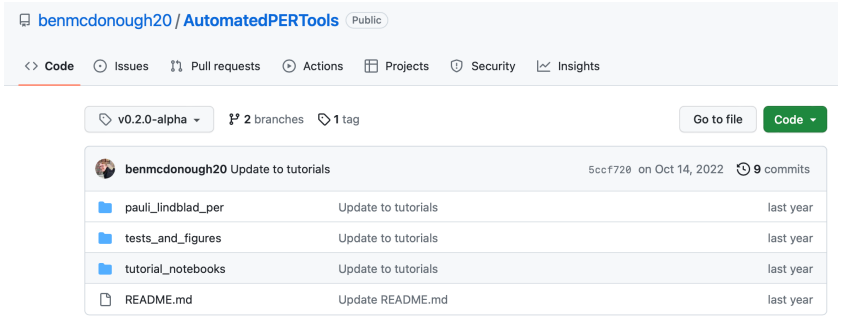

See: B. McDonough et al., 2022 IEEE Workshop on Quantum Computing Software.

Also: arXiv:2210.08611

- Open-source software package that implements Pauli noise tomography and Probabilistic Error Reduction (PER) + Zero Noise Extrapolation
- https://github.com/benmcdonough20/AutomatedPERTools
- Based on Van den Berg *et al.*, Nat. Phys. (2023). Implemented in Qiskit, but not as open-source.

B. McDonough

P. Sharma

Simulating dynamics on quantum computers

Quantum dynamics simulations

Initial state

$$|\Psi(0)\rangle = \sum_n c_n |n\rangle$$

Energy eigenstate of many-body H

Dynamics

$$|\Psi(t)\rangle = \sum_n c_n e^{-iE_n t} |n\rangle$$

Dynamics of an observable O:

$$\langle \mathcal{O}(t) \rangle = \sum_{n,m} c_n c_m^* e^{i(E_m - E_n)t} \langle m|\mathcal{O}|n\rangle$$

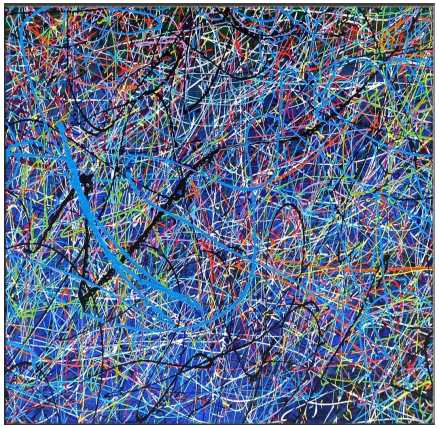

- Classically hard due to rapid growth of entanglement in nonequilibrium for generic H
- Reason: contains highly excited states ➢ Volume-law entanglement entropy

Entanglement = complexity of classical calculation

Exponential growth of classical resources like the bond dimension in tensor networks

Opportunity for quantum computing

Overview of quantum algorithms for dynamics simulations

UNIVERSITÄT DES SAARLANDES

- Lie-Suzuki-Trotter Product formulas (PF)
  - Simple yet limited to early times for current hardware noise
  - Trotter circuit depth scales as $\mathcal{O}(t^{1+1/k})$ ☞ fixed t_{max}
- Algorithms with best asymptotic scaling have significant overhead
  - Linear combination of unitaries (TS) [1], quantum walk methods [2], quantum signal processing (QSP) [3], Lieb-Robinson methods (HHKL) [5]
- Hybrid quantum-classical variational methods [6]
  - Work with fixed gate depth ☞ ideally tailored for NISQ hardware
  - Trading gate depth for doing many QPU measurements
  - Heuristic and may require (exponentially) many parameters

$$H = J\sum_i (Z_i Z_{i+1} + h_i Z_i)$$

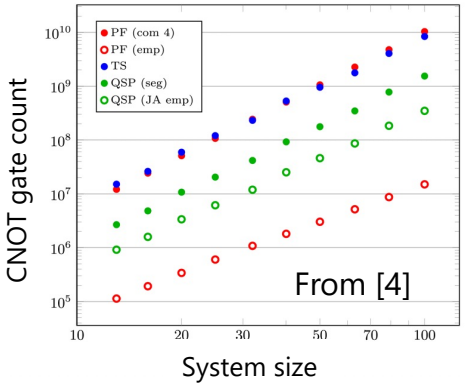

Variational Dynamics Simulations

$$|\Psi[\boldsymbol{\theta}]\rangle = \prod_{\mu=0}^{N_{\boldsymbol{\theta}}-1} e^{-i\theta_\mu \hat{\mathcal{A}}_\mu} |\Psi_0\rangle$$

E.g. MacLachlan principle [6]

$$\sum_\nu M_{\mu\nu}\dot{\theta}_\nu = V_\mu.$$

[1] Berry et al. (2015); [2] Childs (2004); [3] Low, Chuang (2017); [4] Childs et al., PNAS (2018); [5] Haah et al, (2018); [6] Li, Benjamin, Endo, Yuan (2019); Y. Yao, PPO, T. Iadecola *et al.* (2021);
Recent review: Miessen et el., Nature Computational Science (2022).

Overview of methods

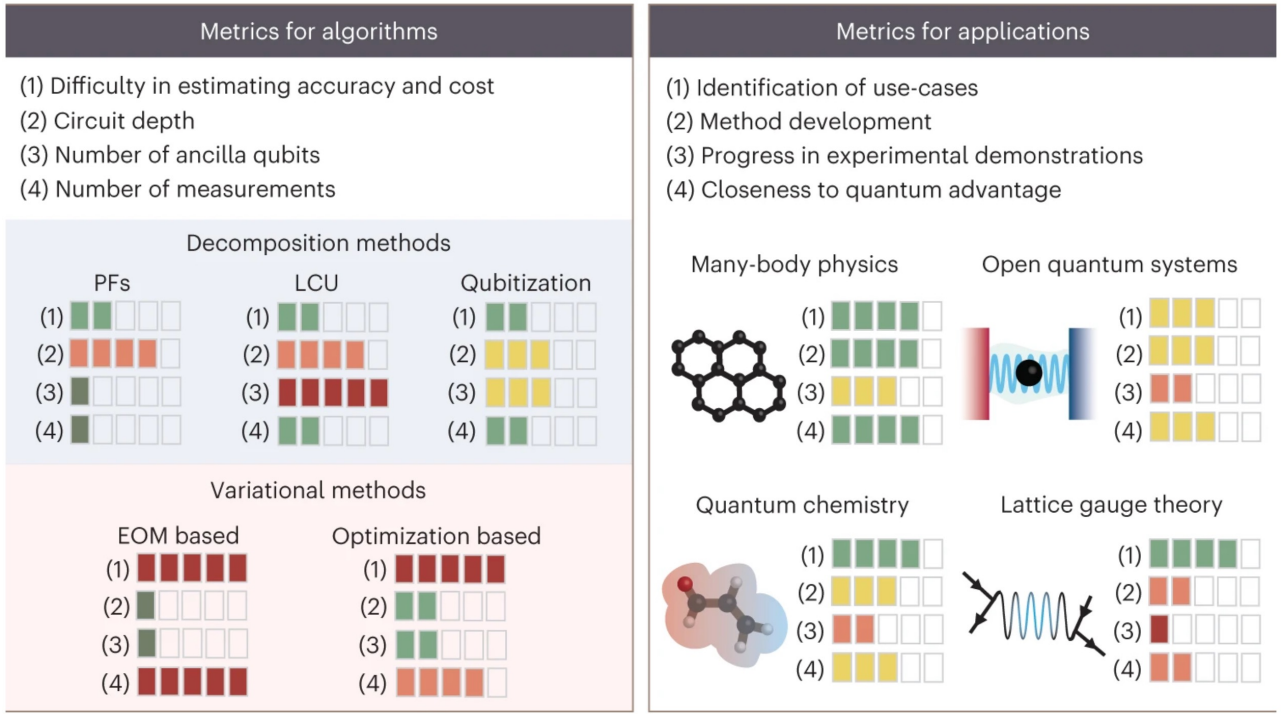

Disclaimer: this can/should be used to start a discussion.

From recent review: Miessen et el., Nature Computational Science (2022).

Overview of methods

Previous work on PFs

- PF for quench dynamics [1] and correlation functions at infinite T [2]
- Combining PFs with VQAs [3]

Previous work on EOM based

- AVQDS (adaptive variational quantum dynamics simulations) [4]
- AVQITE (adaptive variational quantum imaginary time evolution) [5]
- AVQMETTS (adaptive variational quantum minimally entangled typical thermal states) [6]

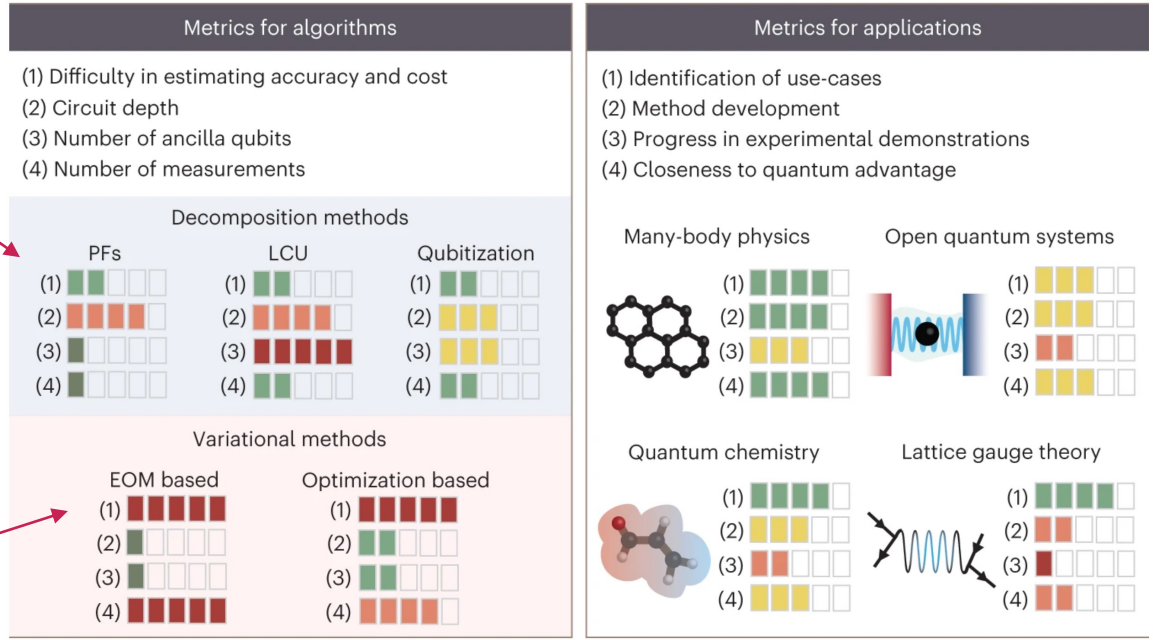

[1] Chen et al., PRR (2022); [2] Chen et al., arXiv (2023); [3] Berthusen et al., PRR (2022); [4] Yao et al., PRX Q (2019); [5] Gomes et al. Adv. QT (2021); [6] Getelina et al., Sci. Post (2023).

Trotter simulations of nonequilibrium dynamics and correlation functions

Trotter simulation of postquench dynamics in MFIM

- Trotter decomposition of time evolution operator $U(t) = e^{-iHt}$
- Decompose Hamiltonian into sum of non-commuting terms
- Example: Mixed-field quantum Ising model

$$H = J \sum_{\langle i,j \rangle} Z_i Z_j + h_x \sum_i X_i + h_z \sum_i Z_i$$

Time evolution operator in 1st order Trotter approximation

$$U(\Delta t) \approx e^{-iH_{ZZ}\Delta t} e^{-iH_Z \Delta t} e^{-iH_X \Delta t}$$

$$R_X(\theta_i^X) = e^{-i\theta_i^X X_i/2}$$

$$R_Z(\theta_i^Z) = e^{-i\theta_i^Z Z_i/2}$$

$$R_{ZZ}(\theta_i^{ZZ}) = e^{-i\theta_i^{ZZ} Z_i Z_{i+1}/2}$$

Standard decomposition of RZZ into CNOT and RZ

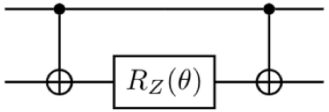

Circuit of single Trotter step for M=5, starting in Neel state.

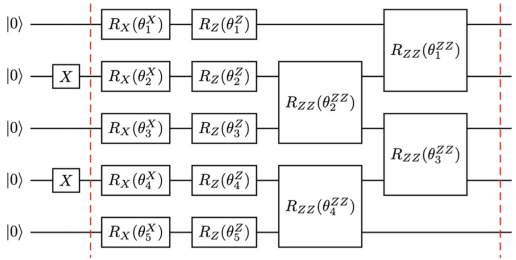

Chen, Burdick, PPO, Iadecola, PRR (2022)

Pulse level control and quantum error mitigation

- Trotter simulation limited to early times by device coherence time
  - Here, 40 Trotter steps on 12 qubits, PBC on `ibmq_guadalupe`
- Pulse level control and quantum error mitigation extend simulation time
  - Direct implementation of RZZ gate using cross-resonance pulse (gate time cut in half)
  - Readout-error mitigation, Zero-noise extrapolation (ZNE) after gate folding (using Mitiq), Pauli twirling
  - Dynamical decoupling
  - Symmetry-based postselection (exact dynamics obeys constraint)

QPU `ibmq_guadalupe`

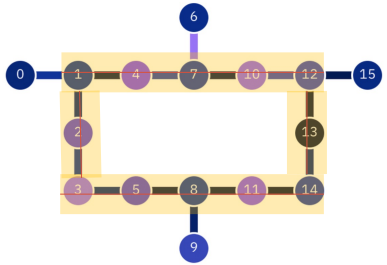

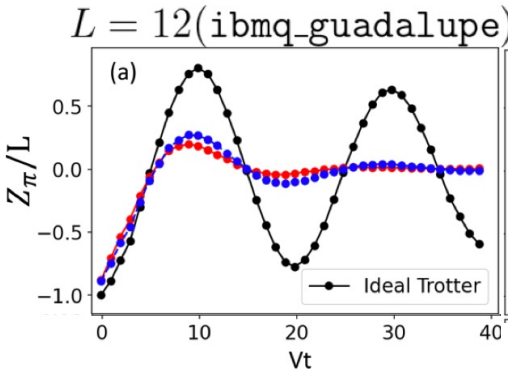

Pulse control

QEM

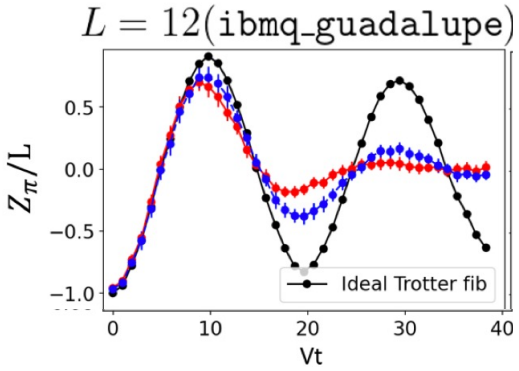

Chen, Burdick, PPO, Iadecola, PRR (2022)

Correlation functions in postquench state

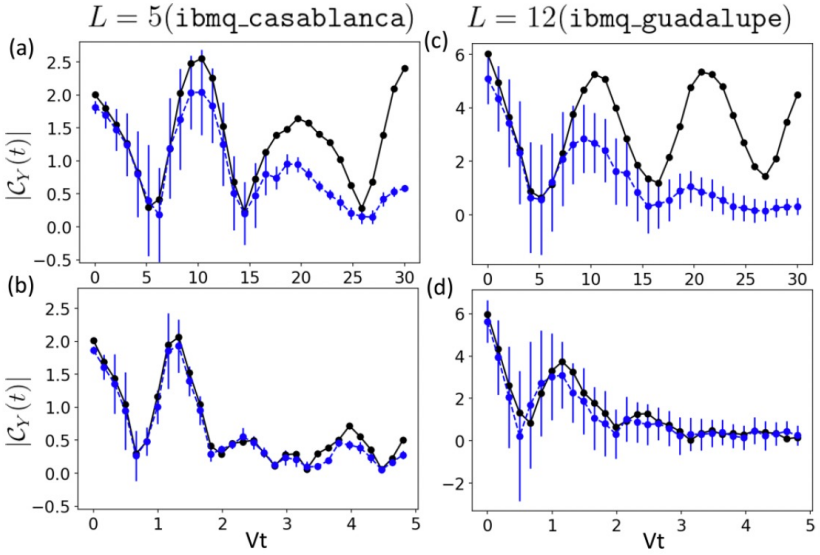

Upper panel: Quantum many-body scar regime $\frac{h_x}{J} = 0.24, \Delta t = 1.$

Lower panel: Chaotic regime $\frac{h_x}{J} = 1, \Delta t = 0.16$

From: Chen, Burdick, PPO, Iadecola, PRR (2022)

- Measure connected correlation function of dressed Y(t) Y(0) operator
- Can use direct measurement circuits [1]
  - 30 Trotter steps, 8192 shots
  - 40000 circuits for 12-qubit system

$$\mathcal{C}_Y(t) = \sum_{i,j} (-1)^{i+j} \langle Z_2 | (PYP)_j(t) (PYP)_i | Z_2 \rangle,$$

$$P_i = (1 + Z_i)/2$$

- Correlator exhibits coherent revivals in scar regime: first revival tracked by QPU

[1] Mitarai, Fujii, PRR (2019)

Method to measure correlation function

$$\mathcal{C}_Y(t) = \sum_j \sum_{i \text{ even}} (-1)^{i+j} \langle Z_2 | (PYP)_j(t) Y_i | Z_2 \rangle. \tag{4.2}$$

It remains to evaluate the local correlators $\langle Z_2 | (PYP)_j(t) Y_i | Z_2 \rangle$. In Ref. [57], it is shown that these can be calculated as

$$\langle Z_2 | (PYP)_j(t) Y_i(0) | Z_2 \rangle = \frac{1}{2}[\langle (PYP)_j(t) \rangle_{M_{Y_i}=1} - \langle (PYP)_j(t) \rangle_{M_{Y_i}=-1}] - \frac{i}{2}[\langle (PYP)_j(t) \rangle_{+Y_i} - \langle (PYP)_j(t) \rangle_{-Y_i}], \tag{4.3a}$$

with

$$\langle (PYP)_j(t) \rangle_{M_{Y_i}=\pm 1} = \frac{1}{2} \langle Z_2 | \left(\frac{I \pm Y_i}{2} \right) U^\dagger(t) (PYP)_j U(t) \left(\frac{I \pm Y_i}{2} \right) | Z_2 \rangle \tag{4.3b}$$

and

$$\langle (PYP)_j(t) \rangle_{\pm Y_i} = \langle Z_2 | e^{\mp i \frac{\pi}{4} Y_i} U^\dagger(t) (PYP)_j U(t) e^{\pm i \frac{\pi}{4} Y_i} | Z_2 \rangle.$$

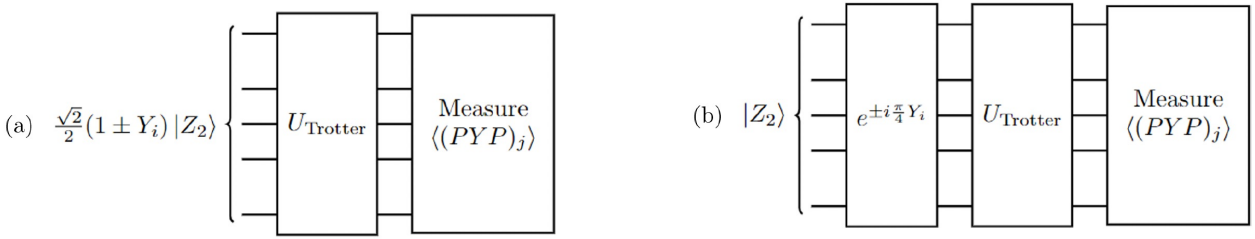

Energy correlation function at infinite temperatures

- MFIM Hamiltonian $H = N\sum_{i=1}^{L} h_i,$ with $h_i = \frac{1}{N}\begin{cases} \Omega X_1 + V Z_1 + \frac{V}{2} Z_1 Z_2 & i = 1 \\ \Omega X_L + V Z_L + \frac{V}{2} Z_{L-1} Z_L & i = L \\ \Omega X_i + 2V Z_i + \frac{V}{2}\left(Z_i Z_{i+1} + Z_{i-1} Z_i\right) & i \neq 1, L \end{cases}$.
- Energy correlator (L = system size)

$$C_r(t) = \langle h_{L/2+r}(t) h_{L/2}(0) \rangle$$

- Normalized correlator

$$\tilde{C}_r(t) = C_r(t)/C$$

$$C = \sum_{r=-L/2+1}^{L/2} C_r(t) = \frac{\Omega^2 + 5V^2}{\Omega^2 + \frac{9}{2}V^2}$$

Chen, Pollock, Yao, PPO, Iadecola, arXiv:2310:03924

Approaches:

- Expectation value in Haar random state (hard on QPU)

$$\langle \psi | Q | \psi \rangle = \langle Q \rangle_\infty + O\left(\frac{\langle Q^\dagger Q \rangle_\infty^{1/2}}{d^{1/2}} \right)$$

$O(1)$ for local correlators

$d = 2^n$

- Sample from y product state basis (easy on QPU)

$$C_r^S(t) = \frac{1}{S}\sum_{k=1}^{S} \mathrm{Re}\,\langle y_k | h_{L/2+r}(t) h_{L/2}(0) | y_k \rangle$$

$$= C_r(t) + O\left(\frac{F_r(L,t)}{S^{1/2}} \right)$$

Std. deviation over all y basis states

Sampling local energy correlation function

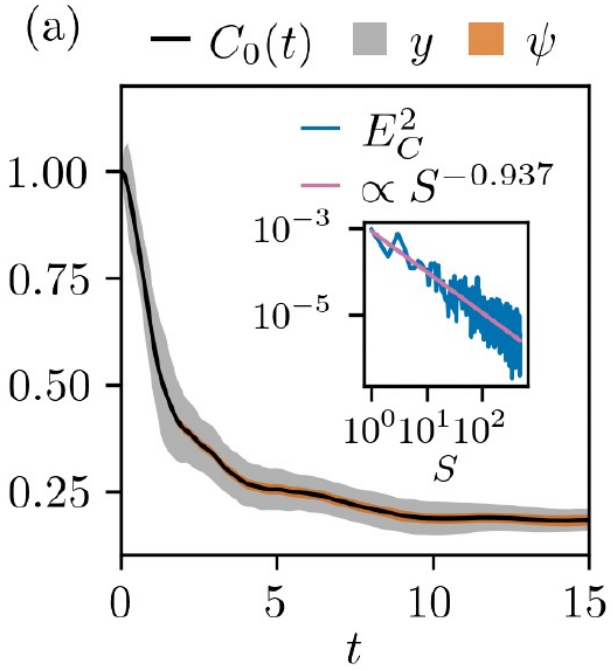

- Average over 1000 Haar random states agrees with exact result
- Grey band shows standard deviation $F_0(L = 12, t)$ of sampling y-product states $|y_k\rangle$
- F_0 is small since random $|y_k\rangle$ look like $T = \infty$ Gibbs states as far as 1. and 2. moment care

$$\langle y|h_i|y\rangle = \langle h_i\rangle_\infty \quad \forall i, y$$
$$\langle y|h_i h_j|y\rangle = \langle h_i h_j\rangle_\infty \quad \forall i, j, y.$$

Chen, Pollock, Yao, PPO, Iadecola, arXiv:2310:03924

Scaling of infinite-T correlator on QPU

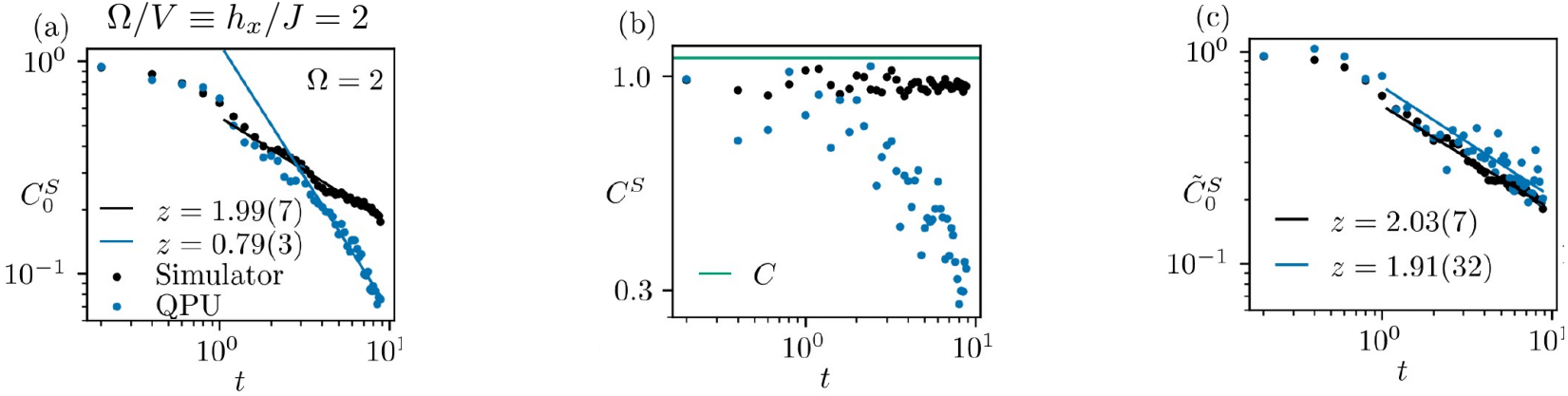

- Direct measurement circuits of correlator [1]: $C_r(t) \sim t^{-1/z}$ Expected z=2 (diffusion) for non-integrable systems
- Average over 12 y-basis states, 90 Trotter steps on `ibm_montreal`.
- Bare correlator shows incorrect scaling exponent due to noise
- Renormalizing correlator with C measured on QPU recovers correct scaling $z = 2$

[1] Mitarai, Fujii, PRR (2019)

Summary and outlook

Thank you for your attention!

UNIVERSITÄT DES SAARLANDES

- Variational quantum algorithms tailored to match quantum resources
  - Main Idea: Create and probe highly entangled state on quantum computer
  - Hard to train expressive states using noisy cost functions: develop VQAs 2.0
- Preload classically trained state on QPU (e.g. MPS), & manipulate further on QPU
- Avoid quantum-classical feedback loop, e.g. using subspace methods
- Trotter simulations utilizing quantum error mitigation are promising to achieve early quantum advantage in simulating dynamics of complex systems

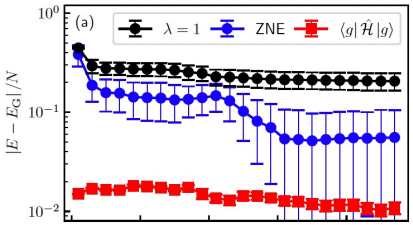

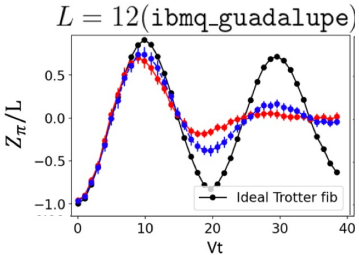

References:

- J. C. Getelina et al., arXiv:2404.09132 (2024).
- A. C. Y. Li et al., Phys. Rev. Research 5, 033071 (2023)
- B. McDonough et al., 2022 IEEE Workshop on QC Software
- I-C. Chen et al., Phys. Rev. Research 4, 043027 (2022)
- I.-C. Chen et al. arXiv:2310:03924

Backup Slides

Details of PER procedure

For PNT, we considered a total of 150 samples for the Pauli twirl consisting of 50 samples for pair-fidelity and 100 single-fidelity. We run circuits of varying depths ([2,4,8,16]) with 1000 shots each to ensure the proper diagonalization of the noise channel. This process generated a Pauli noise model necessary for PER, where we sampled from the partial inverse of the noise model and Pauli twirl. For PER, all 83 commuting Pauli groups are measured with 1000 samples each for five noise strengths $\lambda \in [0, 0.25, 0.5, 0.75, 1, 1.5]$, evaluated with 1000 shots each. This step in the procedure is the most resource-intensive. We then extrapolate each Pauli expectation value to zero noise using the PER results obtained for different noise strengths λ for all measured Pauli groups. These ZNE estimated expectations determine $\mathcal{H}_{ij}$ and $\mathcal{S}_{ij}$, which are used to perform the PIQAE calculation.

Quantum hardware results

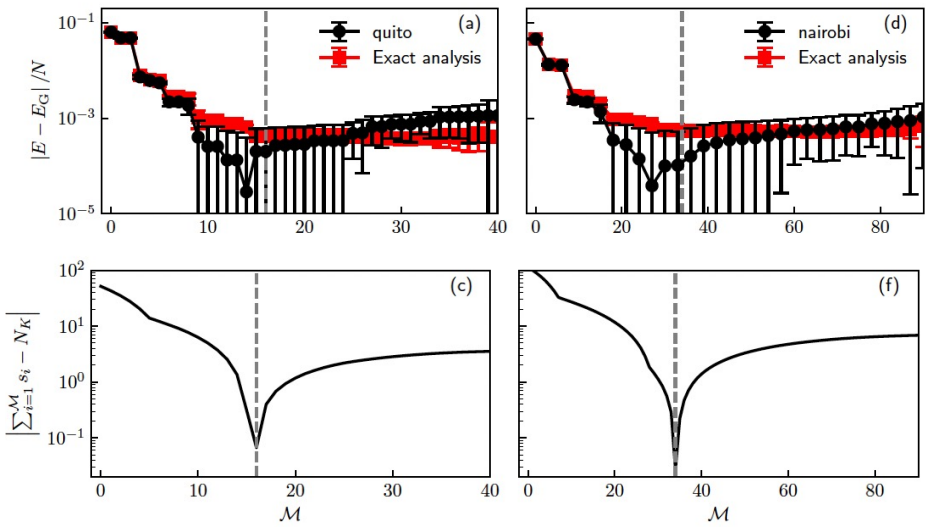

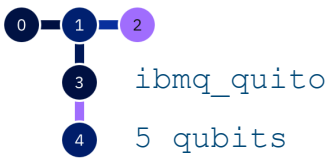

ibmq_quito

5 qubits

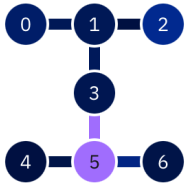

ibmq_nairobi

7 qubits

2^{14} measurement shots. Black error bars are standard error.

- 5 and 7 qubit QPUs
- 1-layer HVA ansatz, K=2 Krylov moment
  → Need to measure up to H^5
- On `ibmq_quito`
  - 822 Pauli strings to measure, 2^{14} shots
  - Dimension FG Krylov space = 82
- On `ibmq_nairobi`
  - 5790 Pauli strings to measure , 2^{14} shots
  - Dimension FG Krylov space = 173
- Use trace condition of overlap matrix to truncate in presence of noise
- Energy converges with error per site < 10^{-3}

16 qubit model on hardware with error mitigation

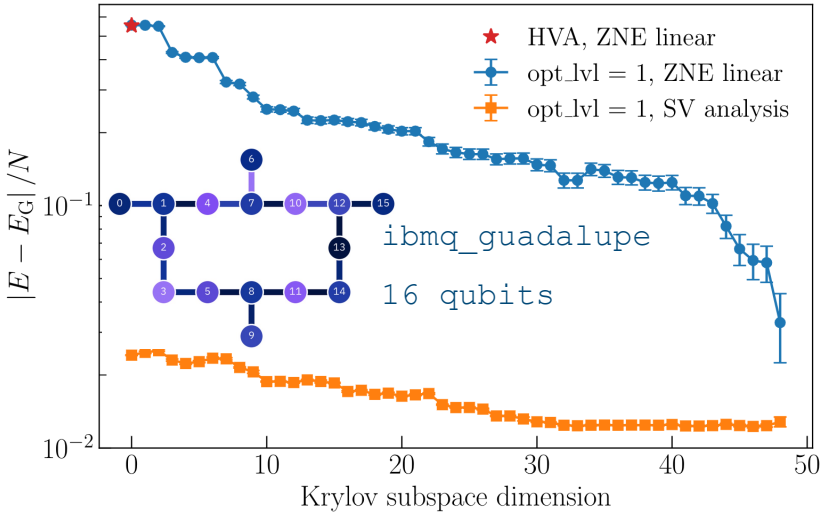

- 16 qubit, MFIM
- 1-layer HVA ansatz, K=1 Krylov moment
- 14'672 Paulis to measure, reduced to 83 noncommuting groups, 2^{14} shots
- Dimension of FG Krylov basis = 49
- ZNE with noise strength $\lambda = \{1.0, 1.5, 2.0\}$ on $\langle H(\lambda)\rangle_{GS(\lambda=1)}$ using linear extrapolation
- Energy converges to exact GS energy up to small error of 3×10^{-2} per site

Next: Estimate resources to scale up to to 127 qubit `ibmq_kyiv` or 433 qubit `ibmq_seattle` QPUs.

Naïve estimate yields 11M Paulis and 62K groups to measure.

For 5×5 TFIM, we find 3.5M Paulis and 2258 groups.

Getelina, PPO et al, (to be submitted)

Correlations at finite temperature

Thermal initial states

Ground State Preparation using VQITE

MacLachlan distance b/w exact and variational time evolution

$$|\Psi[\boldsymbol{\theta}]\rangle = \prod_{\mu=0}^{N_{\boldsymbol{\theta}}-1} e^{-i\theta_\mu \hat{\mathcal{A}}_\mu} |\Psi_0\rangle \quad \Rightarrow \quad \frac{d\rho}{d\tau} = \mathcal{L}_{\text{imag}}(\rho) = -\{H, \rho\} + 2\langle H \rangle \rho \,. \quad \Rightarrow \quad L^2 \equiv \left\| \sum_\mu \frac{\partial \rho[\boldsymbol{\theta}]}{\partial \theta_\mu} \dot{\theta}_\mu - \mathcal{L}_a[\rho] \right\|^2$$

$$= \sum_{\mu,\nu} M_{\mu\nu} \dot{\theta}_\mu \dot{\theta}_\nu - 2 \sum_\mu V_\mu \dot{\theta}_\mu + 2\text{var}_{\boldsymbol{\theta}}[H] \,.$$

Variational parameters evolve in time

Minimize L^2

EOM for variational parameters

$$\sum_\nu M_{\mu\nu} \dot{\theta}_\nu = V_\mu \,.$$

$$M_{\mu\nu} = 2\Re \left[\frac{\partial \langle \Psi[\boldsymbol{\theta}]|}{\partial \theta_\mu} \frac{\partial |\Psi[\boldsymbol{\theta}]\rangle}{\partial \theta_\nu} + \frac{\partial \langle \Psi[\boldsymbol{\theta}]|}{\partial \theta_\mu} |\Psi[\boldsymbol{\theta}]\rangle \frac{\partial \langle \Psi[\boldsymbol{\theta}]|}{\partial \theta_\nu} |\Psi[\boldsymbol{\theta}]\rangle \right]$$

Matrix $M_{\mu\nu}$ and vector V_μ measured on QPU

$$V_\mu = 2\Re \left[-\frac{\partial \langle \Psi[\boldsymbol{\theta}]|}{\partial \theta_\mu} \hat{H} |\Psi[\boldsymbol{\theta}]\rangle \right]$$

Only works when the ansatz can follow the dynamics
☞ How to select an efficient yet flexible variational ansatz?

[1] Motta et al., Nat. Phys. (2020); [2] Lin et al., PRX Q (2022); [3] McArdle et al., npj QI (2019); [4] Gomes, PPO et al., Adv QT (2021)

Trotter dynamics: a path to quantum advantage?

- Recent IBM work demonstrated Trotter dynamics of TFIM on 127 qubits [1]
  - Efficient noise tomography using a sparse Pauli noise model ansatz [2]
  - Precise noise amplification for ZNE since noise is well characterized (see also [3])
- Claimed "quantum utility" regime
  - Spurred classical simulation work [4] that contested that claim (ongoing)
  - Even if this work is not yet beyond classical capabilities, Trotter dynamics is a leading candidate for quantum advantage

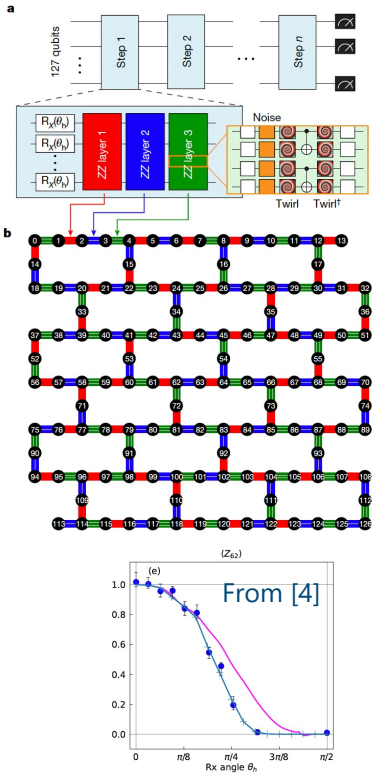

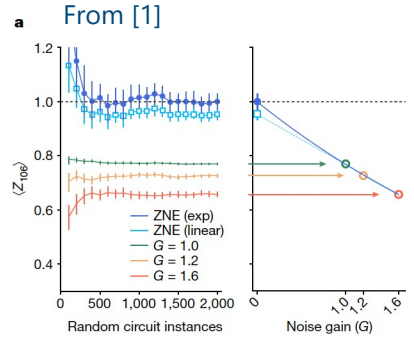

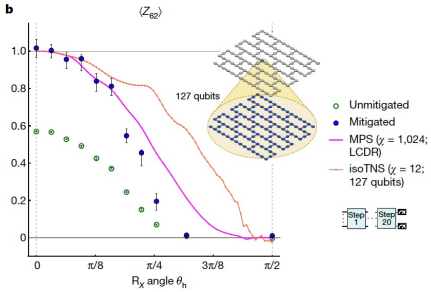

[1] Kim et al. (IBM), Nature (2023); [2] van den Berg et al. (IBM), (2023); [3] McDonough, PPO et al. (2022); [4] Begusic, Chan (2023); Tindall et al. (2023)

Energy transport simulations

- Transport of conserved quantities like energy, charge or spin useful characterization of interacting many-body systems $H = N \sum_i h_i$
- Infinite temperature energy transport $C_r(t) = \langle h_{L/2+r}(t) h_r(0) \rangle \propto t^{-1/z}$
  - Diffusive $z = 2$
- Simulate energy transport of MFIM on `ibmq_montreal` for L=12

Outlook: a quantum computing challenge

- Scaling up simulations into the quantum advantage regime, including scaling of quantum error mitigation methods
- Spatial and temporal fluctuations of qubit characteristics are a challenge
- How do we verify quantum computing results in this regime?

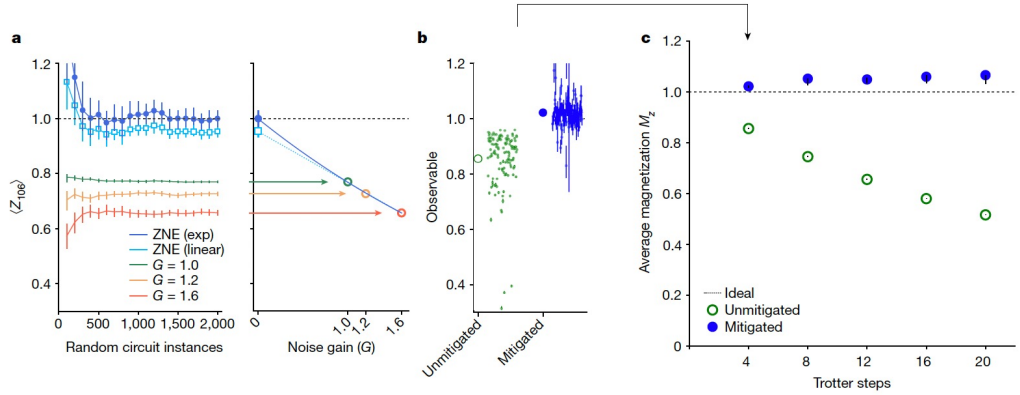

From: Kim et al. (IBM), Nature (2023)

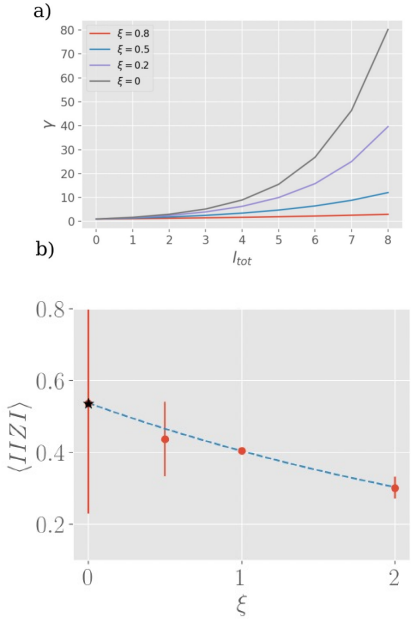

From: McDonough, PPO et al, (2022)

Overview of quantum algorithms for dynamics simulations

- Lie-Suzuki-Trotter Product formulas (PF)
  - Simple yet limited to early times for current hardware noise
  - Trotter circuit depth scales as $\mathcal{O}(t^{1+1/k})$ ☞ fixed t_{max}
- Algorithms with best asymptotic scaling have significant overhead
  - Linear combination of unitaries (TS) [1], quantum walk methods [2], quantum signal processing (QSP) [3], Lieb-Robinson methods (HHKL) [5]
- Hybrid quantum-classical variational methods [6]
  - Work with fixed gate depth ☞ ideally tailored for NISQ hardware
  - Trading gate depth for doing many QPU measurements

Variational Trotter Compression:
Combine simplicity of Trotter product with a variational approach to simulate for long times.

Demonstrate full algorithm on IBM hardware in N. F. Berthusen, PPO et al., PRR (2022).

[1] Berry et al. (2015); [2] Childs (2004); [3] Low, Chuang (2017); [4] Childs et al., PNAS (2018); [5] Haah et al, (2018); [6] Li, Benjamin, Endo, Yuan (2019); Y. Yao, PPO, T. Iadecola *et al.* (2021);
Recent review: Miessen et el., Nature Computational Science (2022).

Variational Trotter Compression (VTC) algorithm

UNIVERSITÄT DES SAARLANDES

- Key idea of VTC algorithm [1, 2, 3]:
  - First, propagate state using Trotter: $|\psi(\boldsymbol{\vartheta}_t)\rangle \longrightarrow U_{\mathrm{trot}}(\tau)\,|\psi(\boldsymbol{\vartheta}_t)\rangle$
  - Then, update variational parameters $\vartheta_t \to \vartheta_{t+\tau}$ by optimizing fidelity cost function

Fidelity cost function

$$\mathcal{C} = |\,\langle\psi_0|U^\dagger(\boldsymbol{\vartheta}_{t+\tau})U_{\mathrm{trot}}(\tau)U(\boldsymbol{\vartheta}_t)|\psi_0\rangle\,|^2$$

Variational state

$$|\psi(\boldsymbol{\vartheta})\rangle = U(\boldsymbol{\vartheta})\,|\psi_0\rangle = \prod_{l=1}^{\ell}\prod_{i=1}^{N} e^{-i\vartheta_{l,i}A_i}\,|\psi_0\rangle$$

ℓ = number of layers
N = number of parameters per layer
A_i = Hermitian operator (e.g. Pauli matrix)

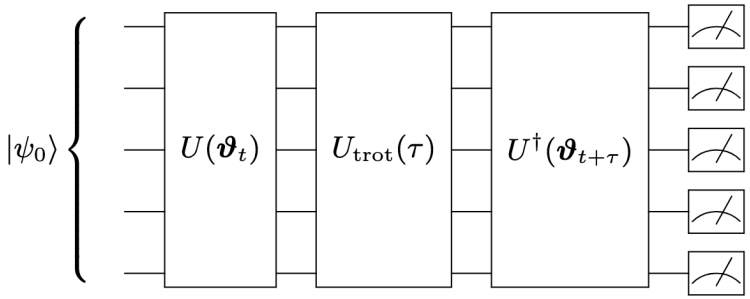

Return probability to initial state is maximal for optimal parameters $\vartheta_{t+\tau}$

Measure cost function on QPU [3]

[1] Lin, Green, Smith, Pollmann (2020); [2] Barison, Carleo (2021), [3] Berthusen, Trevisan, Iadecola, PPO (2022).

Application to Heisenberg model: choice of ansatz

- 1D AF Heisenberg model $H_0 = \frac{J}{4} \sum_{i=1}^{M} (X_i X_{i+1} + Y_i Y_{i+1} + Z_i Z_{i+1})$
- Start from classical Néel state and time-evolve with H_0: $|\psi(t)\rangle = e^{-iH_0 t} |010101\cdots\rangle$

$$|\psi(\boldsymbol{\vartheta}^{(\ell)})\rangle = \prod_{l=1}^{\ell} U_{\text{even}}(\boldsymbol{\phi}_l)\, U_{\text{odd}}(\boldsymbol{\theta}_l)\, |\psi_0\rangle$$

$$U_{\text{odd}}(\boldsymbol{\theta}_l) = \prod_{j \text{ odd}} e^{-i\,\theta_{l,j}\,(X_j X_{j+1} + Y_j Y_{j+1} + Z_j Z_{j+1})}$$

$$U_{\text{even}}(\boldsymbol{\phi}_l) = \prod_{j \text{ even}} e^{-i\,\phi_{l,j}\,(X_j X_{j+1} + Y_j Y_{j+1} + Z_j Z_{j+1})}$$

Brickwall form of quantum circuit

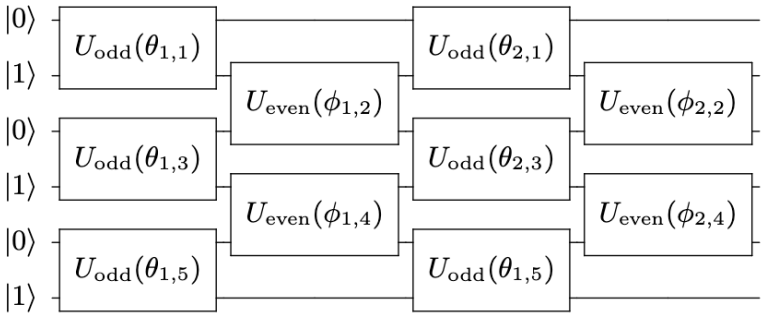

- Determine depth of layered ansatz $\ell \equiv \ell^*$ to accurately describe $|\psi(t)\rangle$

Berthusen, Trevisan, Iadecola, PPO (2022).

Required layer numbers versus time

- Start from classical Néel state and time-evolve with H_0: $|\psi(t)\rangle = e^{-iH_0 t}|010101\cdots\rangle$
- Determine depth of layered ansatz ℓ to accurately describe $|\psi(t)\rangle$

Overlap with exact state

$$1 - \mathcal{F}\left(t, \boldsymbol{\vartheta}^{(\ell)}\right) = 1 - |\langle\psi(\boldsymbol{\vartheta}^{(\ell)})|\psi(t)\rangle|^2$$

Variational form

$$|\psi(\boldsymbol{\vartheta}^{(\ell)})\rangle = \prod_{l=1}^{\ell} U_{\text{even}}(\boldsymbol{\phi}_l)\, U_{\text{odd}}(\boldsymbol{\theta}_l)\, |\psi_0\rangle$$

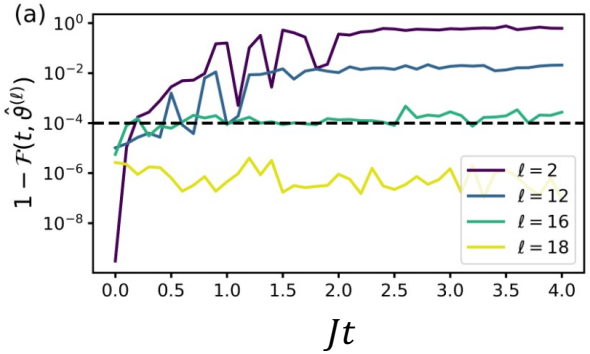

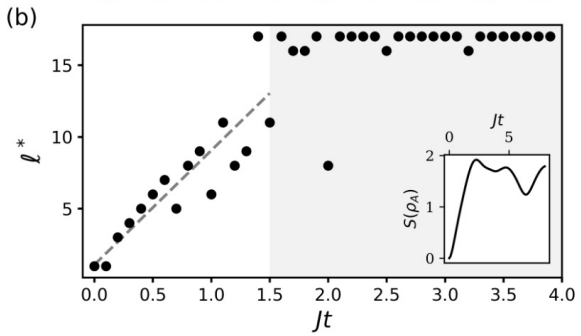

Required layer number ℓ to achieve $1 - \mathcal{F} < 10^{-4}$ grows **linearly with time** and then **saturates**.

VTC benchmark on statevector simulator

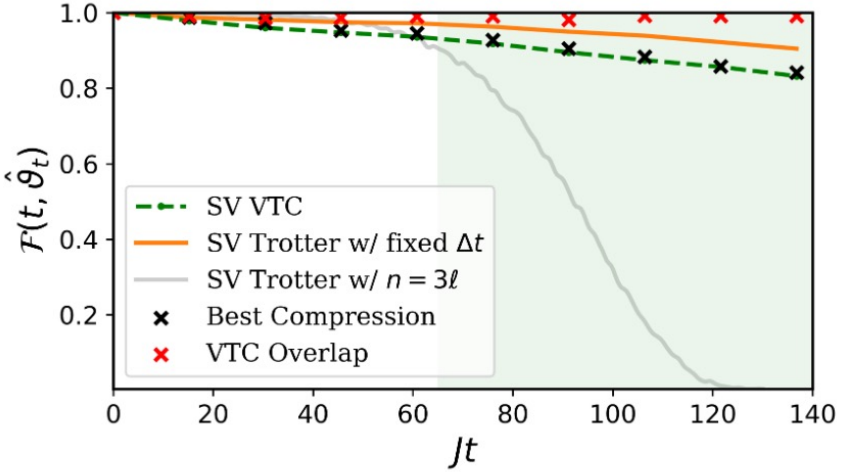

- VTC approximately follows Trotter with fixed small step size $\Delta t = \frac{0.2}{J}$
- Orange curve has depth $n = 700$ at t_f
- Grey curve has depth $3\ell = 228$ at all t
- VTC cost function has fixed depth 3ℓ
- Gradient based optimizer L-BFGS-B

Fidelity = Overlap with exact state $\mathcal{F}(t, \hat{\boldsymbol{\vartheta}}_t) = |\langle\psi(\hat{\boldsymbol{\vartheta}}_t)|\psi(t)\rangle|^2$

$$\text{Best Compression} \equiv |\langle\psi(t)|U_{\text{Trot}}(n=\ell)|\psi(\hat{\boldsymbol{\vartheta}}_{t-\tau})\rangle|^2$$

$$\text{VTC overlap} \equiv |\langle\psi(\hat{\boldsymbol{\vartheta}}_t)|U_{\text{Trot}}|\psi(\hat{\boldsymbol{\vartheta}}_{t-\tau})\rangle|^2$$

VTC allows simulating to arbitrarily long times with high fidelity.

Parameters: $\ell = 76, n = 76$
$\tau = 15.2/J, \Delta t = 0.2/J$

VTC on ideal circuit simulators

- Double-time contour cost function circuit
- Non-gradient-based optimizer: CMA-ES
- Larger shot numbers increase fidelity
- Single compression step takes few hours

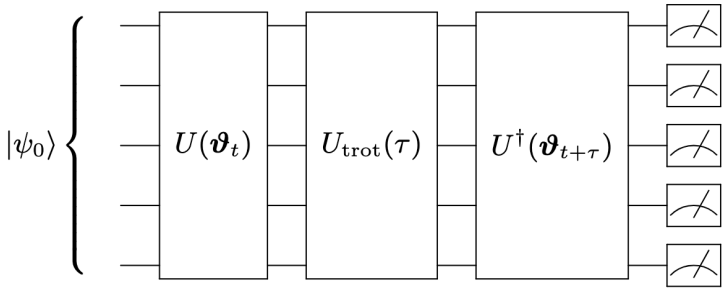

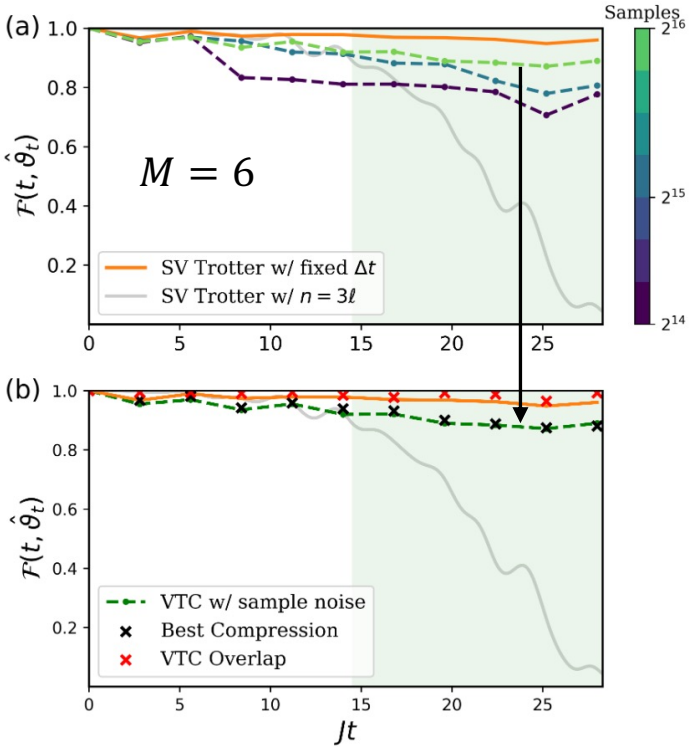

VTC is feasible for noisy cost function

VTC on IBM hardware

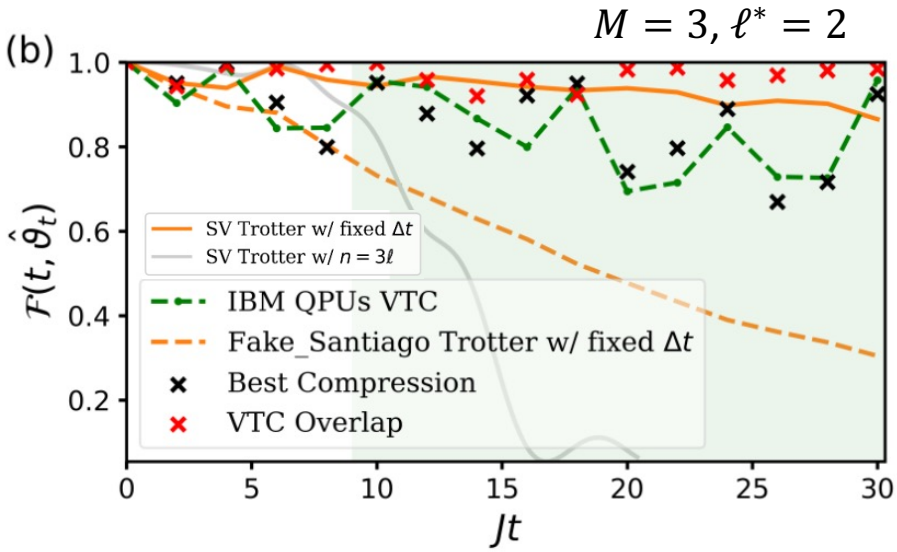

Explicit demonstration of dynamics simulations beyond QPU coherence time

- Cost function evaluation on IBM hardware `ibmq_santiago` & `ibmq_quito`
- Final fidelity = 0.96, where Trotter fidelity has decayed to < 0.4 already
- 15 compression steps
- Average fidelity $\langle F \rangle = 0.86$
- $\mathcal{M} = 5700$ measurement circuits in total
- Comparable number of measurements for MacLachlan simulations $\approx 10^4$

Berthusen, Trevisan, Iadecola, PPO, PRR (2022)

Scaling up nonequilibrium dynamics simulations

- Growth of number of variational parameters with time poses challenge
  - Potential for early/intermediate time dynamics (complexity window) [1]
  - States with low complexity, but long-range entanglement
- Trotter simulations more straightforward to scale up [2]
- Need to be combined with quantum error mitigation (QEM)
  - Controlled QEM requires noise tomography
  - Pauli twirling transforms device noise to Pauli noise [3]
  - Spatially local, Pauli noise tomography is scalable [3, 4, 5]

From: Kim et al. (IBM), Nature (2023)

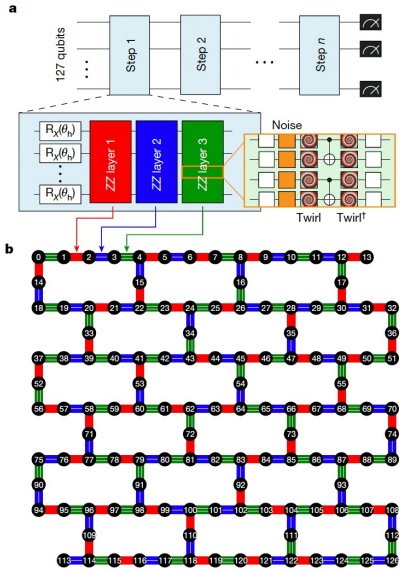

[1] Pollmann et al. (2021) [2] Kim, Wood et al. (IBM) (2023); Chen, PPO et al, (2022); [3] van den Berg et al. (IBM) (2023); Flammia, Wallmann (2019), Cai et al. (2023); [4] Kim et al. (IBM), Nature (2023); [5] McDonough, PPO et al. (2022).

Trotter simulation of postquench dynamics

- Trotter decomposition of time evolution operator $U(t) = e^{-iHt}$
- Decompose Hamiltonian into sum of non-commuting terms
- Example: Mixed-field quantum Ising model

$$H = J \sum_{\langle i,j \rangle} Z_i Z_j + h_x \sum_i X_i + h_z \sum_i Z_i$$

Time evolution operator in 1st order Trotter approximation

$$U(\Delta t) \approx e^{-iH_{ZZ}\Delta t} e^{-iH_Z \Delta t} e^{-iH_X \Delta t}$$

$$R_X(\theta_i^X) = e^{-i\theta_i^X X_i/2}$$

$$R_Z(\theta_i^Z) = e^{-i\theta_i^Z Z_i/2}$$

$$R_{ZZ}(\theta_i^{ZZ}) = e^{-i\theta_i^{ZZ} Z_i Z_{i+1}/2}$$

Standard decomposition of RZZ into CNOT and RZ

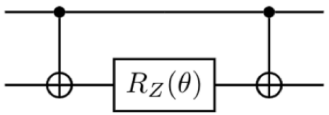

Circuit of single Trotter step for M=5, starting in Neel state.

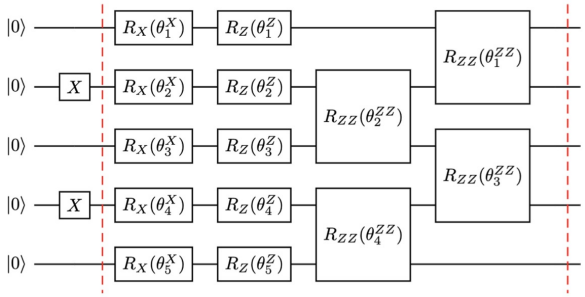

Chen, Burdick, PPO, Iadecola (2022).

Pulse level control and quantum error mitigation

- Trotter simulation limited to early times by device coherence time
- Pulse level control and quantum error mitigation extend simulation time
  - Direct implementation of RZZ gate using cross-resonance pulse (gate time cut in half)
  - Readout-error mitigation, Zero-noise extrapolation (ZNE) after gate folding, Pauli twirling
  - Dynamical decoupling, Symmetry-based postselection (exact dynamics obeys constraint)

QPU `ibmq_guadelupe`
Use 12 qubits, PBC,
40 Trotter steps

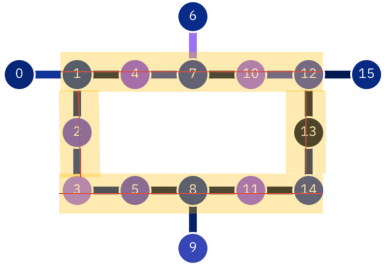

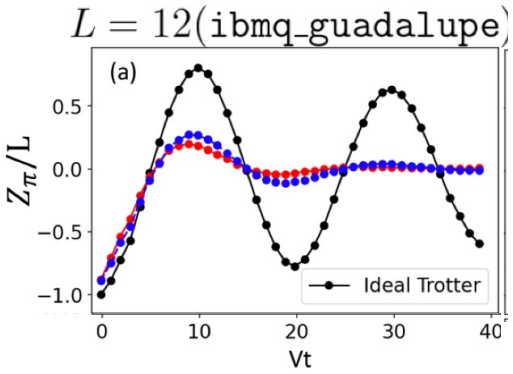

Pulse control

QEM

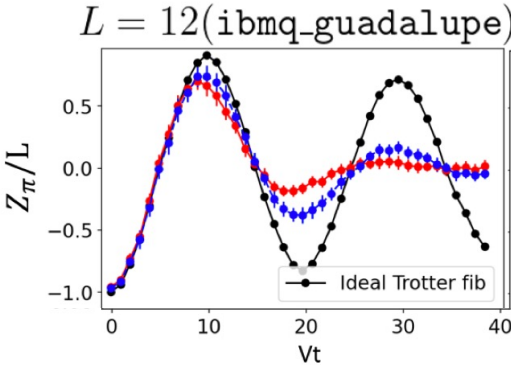

Chen, Burdick, PPO, Iadecola (2022).

Quantum Error Mitigation using quasiprobability methods

Motivation and Take-Home Messages

- Current quantum hardware experiences significant levels of noise
  - How can we mitigate the effects of noise on quantum computations?
  - Can we exploit the presence of noise when simulating open (ie noisy) quantum systems?
- Quasiprobability methods are systematic approach of removing noise induced bias
  - Probabilistic Error Cancellation (PEC) [1] trades bias reduction for increased variance
  - Incurs exponentially large classical sampling overhead $\propto$ noise strength, circuit depth
  - Probabilistic Error Reduction (PER) [2] alleviates sampling overhead by reducing noise only partially $\rightarrow$ combined with extrapolation can yield results comparable to PEC
- Inherent device noise can act as resource in simulations of open quantum systems
  - Device noise can reduce the sampling overhead if somewhat close to what you want to simulate [3]
  - Only some type of noise acts as a resource (e.g. non-unital noise)

[1] Temme et al. (2017); Endo et al. (2017); [2] Mari et el. (2021); McDonough, PPO et al. (2022); [3] Aftergood, PPO et al. (to be submitted); Guimarães et al. (2023)

Ideal circuit evaluation of expectation value

- Applicable to algorithms in which the figure of merit is an expectation value averaged over many shots of a unitary circuit

Ideal circuit

Input state is prepared

ρ_0

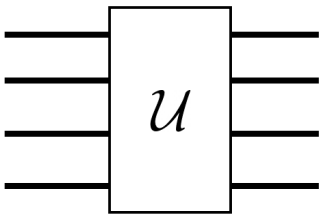

One or more expectation values are obtained

$\langle \mathcal{O} \rangle_{\text{ideal}} = \text{Tr}[\mathcal{O}\mathcal{U}(\rho_0)]$

A unitary circuit is run

$$\mathcal{U}(\rho_0) = (\mathcal{U}_l \circ \ldots \circ \mathcal{U}_1)(\rho_0)$$

[1] Temme et al. (2017); Endo et al. (2018); [2] van den Berg et al. (2023); Cai et al. (2023).

Noisy expectation value from noisy quantum circuit

- Noise introduces bias into the estimator of this expectation value.

Noisy circuit

State preparation error affects input state

$\tilde{\rho}_0$

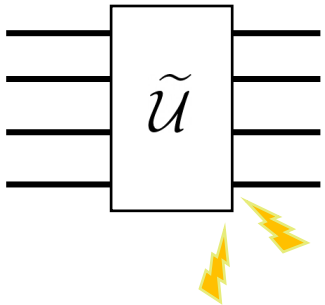

Measurement error also adds to noise in final expectation value

$$\langle \mathcal{O} \rangle = \mathrm{Tr}[\tilde{\mathcal{O}}\tilde{\mathcal{U}}(\rho_0)]$$

Circuit is non-unitary $\tilde{\mathcal{U}} = \tilde{\mathcal{U}}_l \circ \ldots \circ \tilde{\mathcal{U}}_1$ with $\tilde{\mathcal{U}}_i = \Lambda_i \circ \mathcal{U}_i$

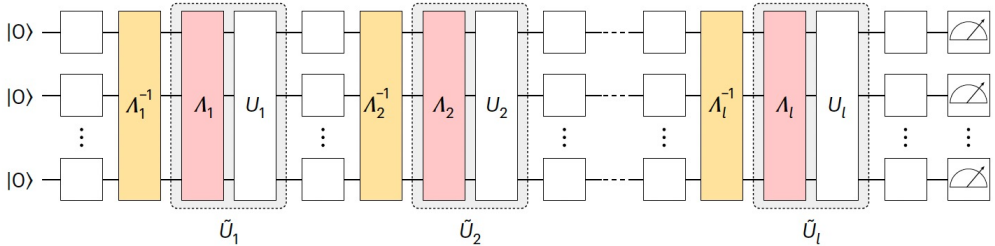

From van den Berg et al. (2023).

Ideal expectation value as linear combination of noisy circuits

- After characterizing the noisy operations $\{G_\alpha\}$, the ideal circuit is decomposed into $\mathcal{U}(\rho) = \sum_\alpha \eta_\alpha G_\alpha(\rho)$ with real coefficients η_α.
- Linearity of the expectation value allows writing the ideal value as $\langle O \rangle_{ideal} = \sum_\alpha \eta_\alpha \langle O \rangle_\alpha$

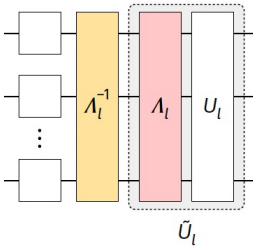

$$\mathcal{U}_l = \Lambda_l^{-1} \circ \tilde{\mathcal{U}}_l = \sum_k \eta_{l,k} \mathcal{G}_k$$

Inverse channel is not physical.
Thus implemented on average by classical postprocessing.

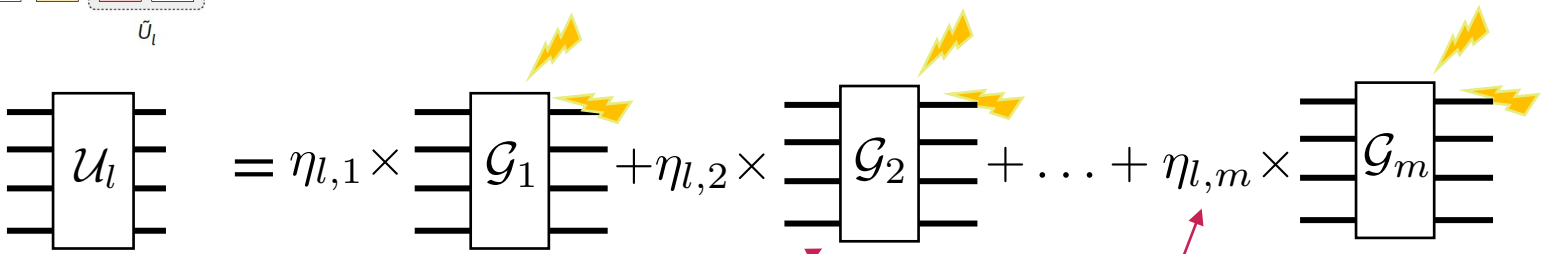

Ideal (noiseless) circuit layer

Noisy circuits

Real, possibly negative coefficients

Exponential sampling overhead due to negativity

- Number of terms grows exponentially with circuit depth l

$$\mathrm{Tr}[\mathcal{O}(\mathcal{U}_l \circ \ldots \circ \mathcal{U}_1)(\rho_0)] = \sum_{k_1,\ldots,k_l} \eta_{1,k_1} \cdots \eta_{l,k_l} \mathrm{Tr}[\mathcal{O}(G_{l,k_l} \circ \ldots \circ G_{1,k_1})(\rho_0)]$$

- The linear combination is converted to a quasiprobability distribution (QPD) and sampled

$$\mathrm{Tr}[\mathcal{O}(\mathcal{U}_l \circ \ldots \circ \mathcal{U}_1)(\rho_0)] = \gamma_1 \cdots \gamma_l \sum_{k_1,\ldots,k_l} \mathrm{sgn}(\eta_{1,k_1}) \cdots \mathrm{sgn}(\eta_{l,k_l}) \frac{|\eta_{1,k_1}|}{\gamma_1} \cdots \frac{|\eta_{l,k_l}|}{\gamma_l} \mathrm{Tr}[\mathcal{O}(G_{l,k_l} \circ \ldots \circ G_{1,k_1})(\rho_0)]$$

Increased range ☞ increased variance $\Delta\mathcal{O}^2 \propto \gamma^2$

Obtain via Monte Carlo sampling

Sample

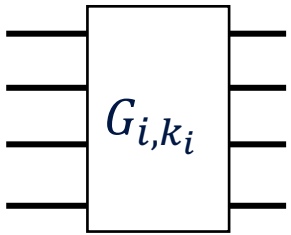

with probability $\frac{|\eta_{i,k_i}|}{\gamma_i}$

Then, scale expectation value by $\gamma_i \, \mathrm{sgn}(\eta_{i,k_i})$ with $\gamma_i = \sum_{k_i} |\eta_{i,k_i}| \geq 1$

Sampling overhead due to negative volume of QPD ∝ noise strength

Example: Pauli noise

- Transform hardware noise to Pauli noise by Pauli twirling $\Lambda_{\mathcal{P}} = \frac{1}{|\mathcal{P}|} \sum_a \mathcal{P}_a \Lambda \mathcal{P}_a$
  - Works only for layers composed of Clifford gates
  - Assumes dominant noise source are CNOT gates

$$\sum_a (\mathcal{P}_a^C \mathcal{C} \Lambda \mathcal{P}_a)(\rho) = \sum_{a,\nu} \underbrace{P_a^C C} M_\nu P_a \rho P_a^\dagger M_\nu^\dagger C^\dagger (P_a^C)^\dagger = (\Lambda_{\mathcal{P}} \mathcal{C})(\rho)$$

$$= C P_a$$

Randomly sampled Pauli gates

Conjugate Pauli operators

$$C P_a C^\dagger = P_a^C$$

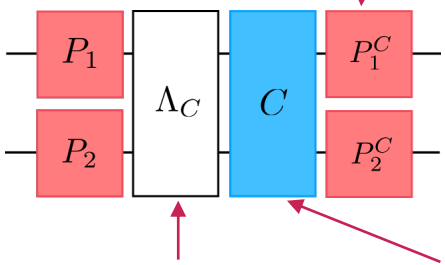

Noise associated with layer

Clifford layer

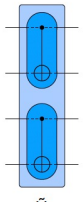

Dressing noise by random Paulis diagonalizes Λ in the Pauli basis

[1] van den Berg et al. (2023); Flammia, Wallmann (2019)

Sparse Pauli-Lindblad noise model

- Sparse Pauli noise model parameters λ_k of a given layer can be efficiently learned [1,2]

Lindbladian $\mathcal{L}(\rho) = \sum_k \lambda_k (P_k \rho P_k - \rho)$ [1] van den Berg et al. (2023); Flammia, Wallmann (2019)

Pauli noise channel $\Lambda(\rho) = e^{\mathcal{L}}(\rho) = \prod_k [w_k(\cdot) + (1 - w_k) P_k(\cdot) P_k](\rho)$

Noise coefficients $w_k = \frac{1}{2}(1 + e^{-2\lambda_k}) \approx 1 - 2\lambda_k$

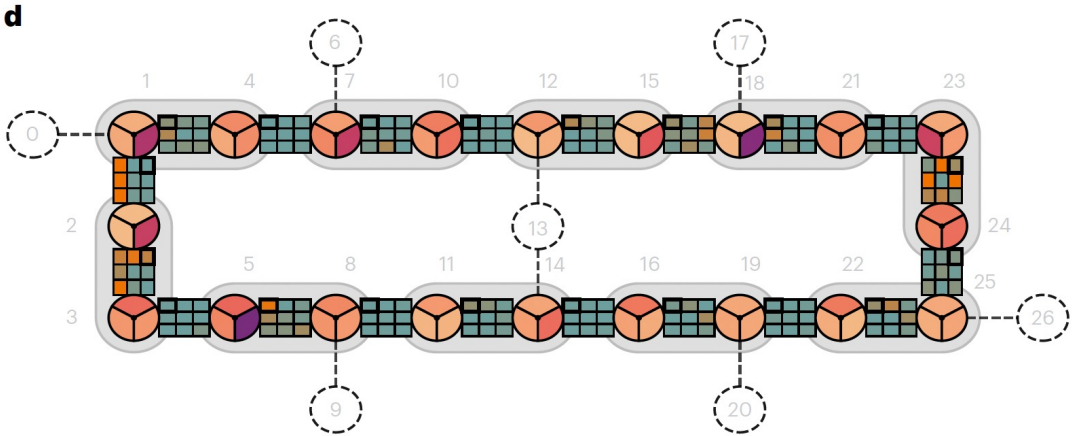

From van den Berg et al. (2023)

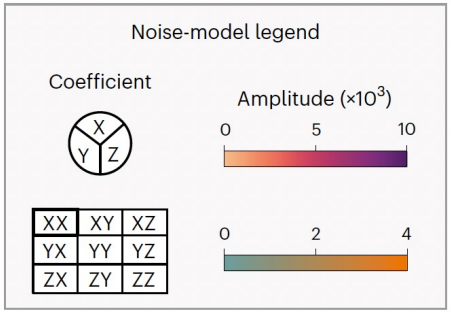

Sparse Pauli-Lindblad noise model

- Sparse Pauli noise model parameters λ_k of a given layer i can be efficiently learned [1,2]

Lindbladian $\mathcal{L}(\rho) = \sum_k \lambda_k (P_k \rho P_k - \rho)$

Pauli noise channel $\Lambda(\rho) = e^{\mathcal{L}}(\rho) = \prod_k [w_k(\cdot) + (1 - w_k) P_k(\cdot) P_k](\rho)$

$\gamma_i = e^{2 \sum_k \lambda_k} \geq 1$

Inverse map $\Lambda^{-1}(\rho) = e^{-\mathcal{L}}(\rho) = \gamma_i \prod_k [w_k(\cdot) - (1 - w_k) P_k(\cdot) P_k](\rho)$

[1] van den Berg et al. (2023); Flammia, Wallmann (2019)

PEC at work: Trotterized time evolution

McDonough, PPO et al, IEEE (2022).

Algorithm 1 Description of PER routine

Input: Circuit with layers $l \in \{1, .., l_{tot}\}$, each with noise model parameters $\{w_{l1}^{(\xi)}, ..., w_{ln}^{(\xi)}\}$

Output: A sample of the PER expectation value (before readout error mitigation)

```
Let α ≡ 1
for l ∈ {1, ..., l_tot} do
    Compose layer l into circuit
    for k ∈ {1, ..., n} do
        Sample I with probability w_lk^(ξ) and P_k otherwise
        Multiply α by γ_l^(ξ)
        if P_k was sampled then
            Multiply α by −1
        end if
        Compose sampled operator into circuit
    end for
end for
Run the circuit and get the expectation value
if ξ < 1 then
    Scale result by α
end if
```

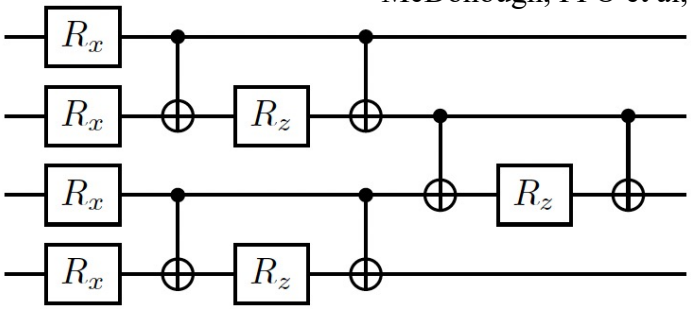

Fig. 7: The realization of a single Trotter step as a quantum circuit. Here we have defined $R_x \equiv RX(-2h\delta t)$ and $R_z \equiv RZ(2J\delta t)$

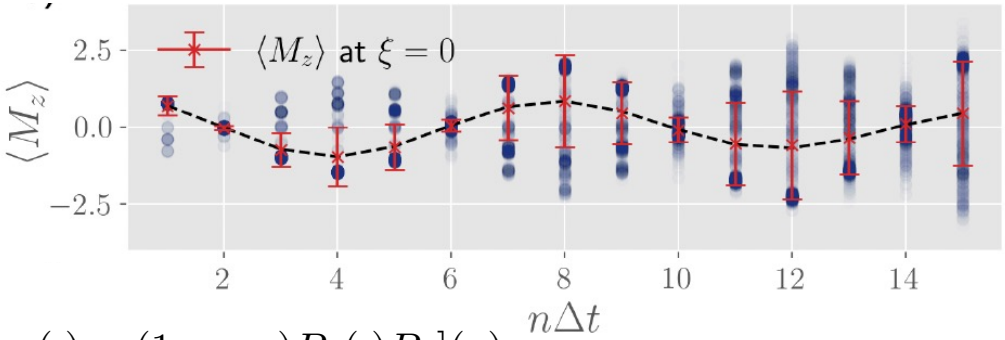

Inverse map $\Lambda^{-1}(\rho) = e^{-\mathcal{L}}(\rho) = \gamma_i \prod_k [w_k(\cdot) - (1 - w_k)P_k(\cdot)P_k](\rho)$

Probabilistic Error Reduction (PER)

Mari et al. (2021); McDonough, PPO et al, IEEE (2022).

- PEC sampling overhead increases exponentially with noise strength x depth
- Remove noise only partially to reduce overhead

$$\gamma = (\gamma_0)^l$$

- $$\Lambda^{(\xi)} = \gamma^{(\xi)} \prod_k \left(w_k^{(\xi)} \mathcal{I} + \mathrm{sgn}(\xi - 1)(1 - w_k^{(\xi)}) \mathcal{P}_k \right). \quad (11)$$

Here, $w^{(\xi)} \equiv \frac{1}{2}(1 + e^{-2|1-\xi|\lambda_k})$ and the sampling overhead

$$\gamma^{(\xi)} = \begin{cases} \exp[2(1-\xi)\sum_k \lambda_k] & \xi < 1 \\ 1 & \xi \geq 1 \end{cases} \quad (12)$$

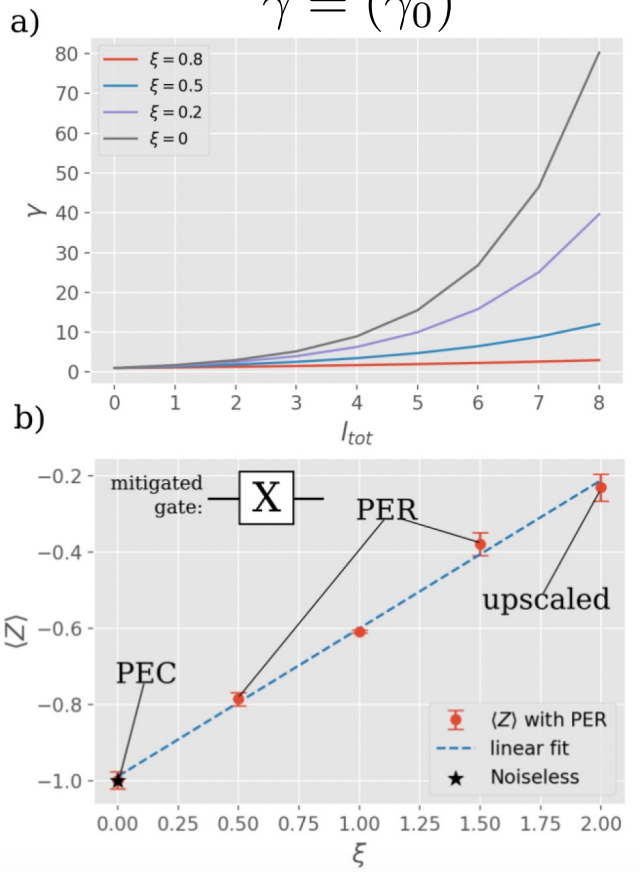

Example: error mitigation on single X gate on Rigetti hardware. Obtained noise model using Gate Set Tomography (GST): $\gamma_0 = 1.73$

PER + vZNE reduces sampling overhead

McDonough, PPO et al, IEEE (2022).

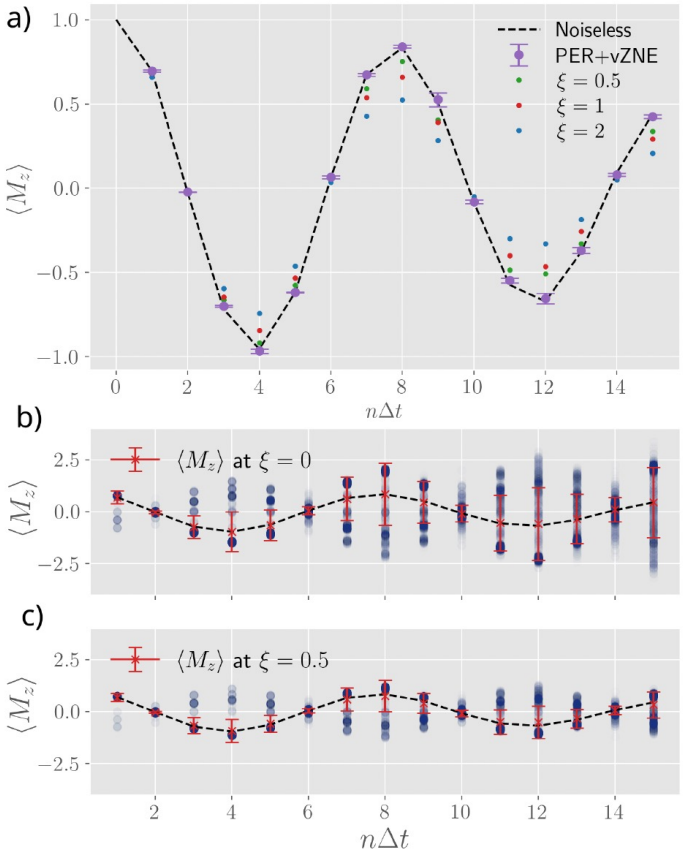

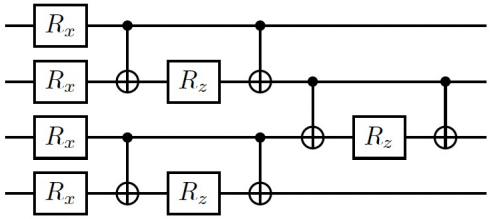

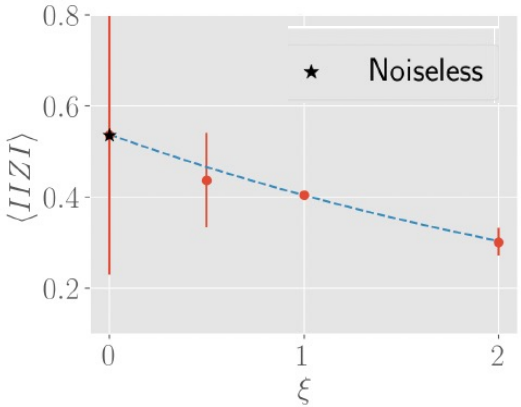

Scaling up noise using this method has been used in recent IBM "quantum utility" work: Kim et al. Nature (2023).

Open source software for automated error mitigation

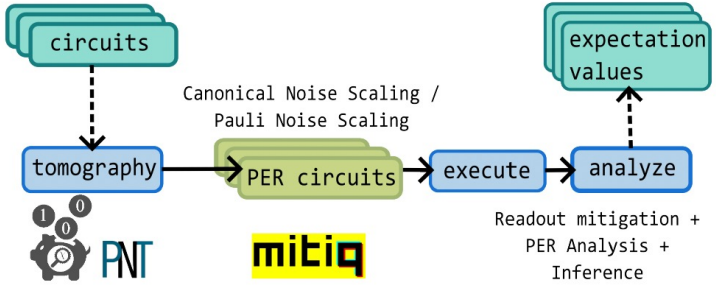

Fig. 1: Illustration of automated error mitigation protocol starting from user defined circuits and returning noise-mitigated expectation values. It includes a noise tomography step involving PNT or GST, whose results are used to generate sampled PER circuits via canonical or Pauli noise scaling.

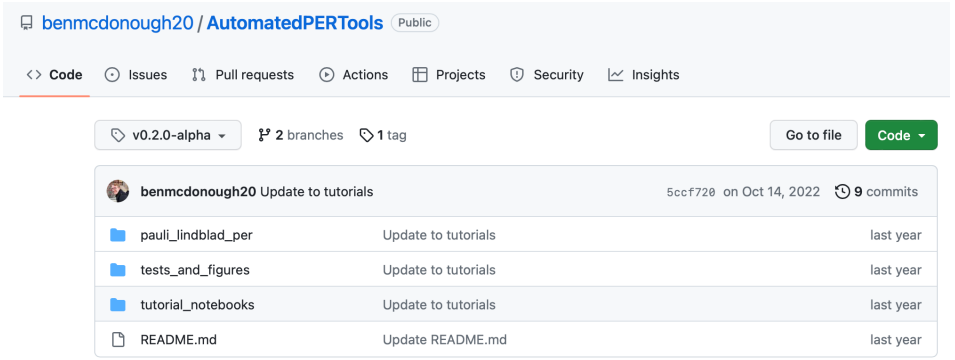

- Open source software package that implements Pauli noise tomography and Probabilistic Error Reduction + Zero Noise Extrapolation
- https://github.com/benmcdonough20/AutomatedPERTools
- Similar method has been implemented by IBM in Qiskit, but source code is not openly accessible

Trotter dynamics: a path to quantum advantage?

- Recent IBM work demonstrated Trotter dynamics of TFIM on 127 qubits [1]
  - Efficient noise tomography using a sparse Pauli noise model ansatz [2]
  - Precise noise amplification for ZNE since noise is well characterized (see also [3])
- Claimed "quantum utility" regime
  - Spurred classical simulation work [4] that contested that claim (ongoing)
  - Even if this work is not yet beyond classical capabilities, Trotter dynamics is a leading candidate for quantum advantage

From [1]

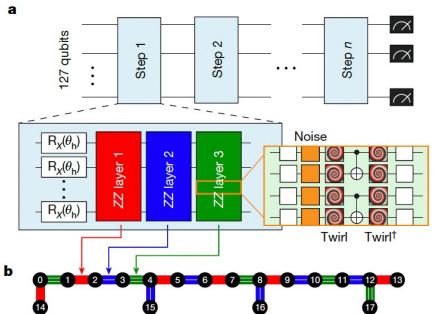

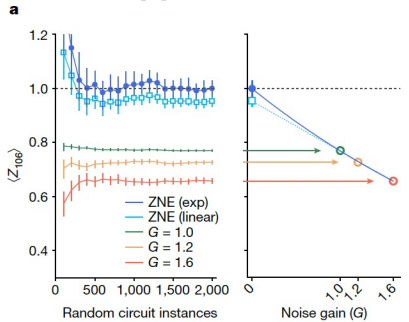

[1] Kim et al. (IBM), Nature (2023); [2] van den Berg et al. (IBM), (2023); [3] McDonough, PPO et al. (2022); [4] Begusic, Chan (2023); Tindall et al. (2023)

Summary

- Variational quantum algorithms tailored to match quantum resources
  - Main Idea: Create and probe highly entangled state on quantum computer
- Quantum-classical feedback loop can be avoided
- Flexible choice of cost functions produces different states
- Main challenges for scaling up system sizes
  - Noisy classical optimization in feedback loop
  - Large number of variational parameters
  - Large number of measurements
- Trotter simulations utilizing quantum error mitigation are primary contender for early quantum advantage

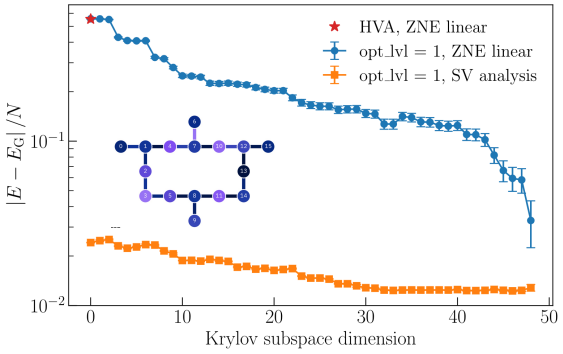

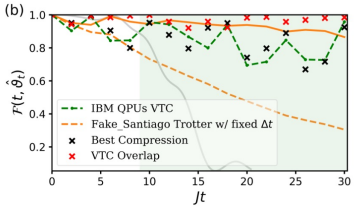

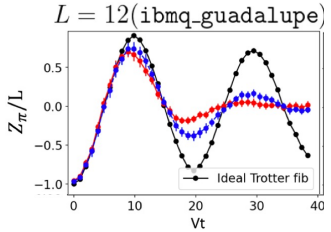

References:

- A. C. Y. Li, PPO *et al.*, Phys. Rev. Research (2023)
- N. F. Berthusen, PPO *et al.*, Phys. Rev. Research (2022)
- I-C. Chen, PPO *et al.*, Phys. Rev. Research (2022)
- B. McDonough, PPO *et al.*, 2022 IEEE Workshop